

Monitoring of Indoor Air Quality at a Large Sailing Cruise Ship to Assess Ventilation Performance and Disease Transmission Risk

Ho Yin Wickson Cheung^a, Prashant Kumar^{a,b,*}, Sarkawt Hama^a, Ana Paula Mendes Emygdio^{a,c}, Yingyue Wei^a, Lemonia Anagnostopoulos^d, John Ewer^e, Valerio Ferracci^c, Edwin R Galea^e, Angus Grandison^e, Christos Hadjichristodoulou^d, Fuchen Jia^e, Pierfrancesco Lepore^f, Lidia Morawska^{a,g}, Varvara A Mouchtouri^d, Niko Siilin^h, Zhaozhi Wang^e, for the HEALTHY SAILING projectⁱ

^a*Global Centre for Clean Air Research (GCARE), Department of Civil and Environmental Engineering, Faculty of Engineering and Physical Sciences, University of Surrey, Guildford GU2 7XH, United Kingdom*

^b*Institute for Sustainability, University of Surrey, Guildford GU2 7XH, United Kingdom*

^c*National Physical Laboratory (NPL), Atmospheric Environmental Science Department, Hampton Road, Teddington, Middlesex TW11 0LW, United Kingdom*

^d*Laboratory of Hygiene and Epidemiology, Faculty of Medicine, University of Thessaly, Larissa 41222, Greece*

^e*Centre for Safety, Resilience and Protective Security, Fire Safety Engineering Group, School of Computing and Mathematical Sciences, Faculty of Engineering and Science, University of Greenwich, Greenwich SE10 9LS, United Kingdom*

^f*Public Health and Medical Public Affairs, MSC Cruise Management, Uxbridge UB11 1AF, United Kingdom*

^g*International Laboratory for Air Quality and Health (ILAQH), School of Earth and Atmospheric Sciences, Faculty of Science, Queensland University of Technology, Queensland 4000, Australia*

^h*VTT Technical Research Centre of Finland Ltd, Espoo 02150, Finland*

ⁱthe HEALTHY SAILING project in collaborators listed in the [Appendix](#) section.

*Corresponding author: Address as above. Email p.kumar@surrey.ac.uk (Prashant Kumar)

Graphical abstract



Abstract

Large passenger ships are characterised as enclosed and crowded indoor spaces with frequent interactions between travellers, providing conditions that facilitate disease transmission. This study aims to provide an indoor ship CO₂ dataset for inferring thermal comfort, ventilation and infectious disease transmission risk evaluation. Indoor air quality (IAQ) monitoring was conducted in nine environments (three cabins, buffet, gym, bar, restaurant, pub and theatre), on board a cruise ship voyaging across the UK and EU, with the study conducted in the framework of the EU HEALTHY SAILING project. CO₂ concentrations, temperature and relative humidity (RH) were simultaneously monitored to investigate thermal characteristics and effectiveness of ventilation performance. Results show a slightly higher RH of $68.2 \pm 5.3\%$ aboard compared to ASHRAE and ISO recommended targets, with temperature recorded at $22.3 \pm 1.4^\circ\text{C}$. Generally, good IAQ (<1000 ppm) was measured with CO₂ mainly varying between 400-1200 ppm. The estimated air change rates (ACH) and ventilation rates (VR)

implied sufficient ventilation was provided in most locations, and the theatre (VR: 86 L s⁻¹ person⁻¹) and cabins (VR: >20 L s⁻¹ person⁻¹) were highly over-ventilated. Dining areas including the pub and restaurant recorded high CO₂ concentrations (>2000 ppm) potentially due to higher footfall (0.6 person/m² and 0.4 person/m²) and limited ACH (2.3 h⁻¹ and 0.8 h⁻¹), indicating a potential risk of infection; these areas should be prioritised for improvement. The IAQ and probability of infection indicate there is an opportunity for energy saving by lowering hotel load for the theatre and cabins and achieving the minimum acceptable VR (10 L s⁻¹ person⁻¹) for occupants' comfort and disease control. Our study produced a first-time dataset from a sailing cruise ship's ventilated areas and provided evidence that can inform guidelines about the optimisation of ventilation operations in large passenger ships, contributing to respiratory health, infection control and energy efficiency aboard.

Keywords: Cruise ship; Ventilation; Indoor air quality; Thermal comfort; Infectious transmission risk; CO₂

1. Introduction

At the beginning of the COVID-19 pandemic, mass gathering events were suspected to provide conditions for the transmission of severe acute respiratory syndrome coronavirus 2 (SARS-CoV-2) virus and pose severe challenges to public health authorities. In the face of the widespread COVID-19 pandemic, governments around the world called for the suspension of gatherings, introducing travel restrictions, entry bans, isolation and quarantine to reduce physical contact and interaction of people which facilitates virus transmission. However, these travel restrictions brought public concerns, due to self-isolation and self-distancing rules as well as significant economic losses to the global tourism industry (UNWTO, 2021). During the pandemic, international transport including air and land (rail/road) transports was restricted to only essential activities. Regarding maritime transport, as one of the early SARS-CoV-2

outbreaks on board a cruise ship, the outbreak unfolding onboard Diamond Princess brought COVID-19 to the sight of the cruise industry and public. The Diamond Princess was placed under quarantine at Yokohama port in Japan for nearly a month, with onboard quarantine of passengers and crew members except when performing essential duties. The outbreak resulted in 712 COVID-19 cases and 13 deaths (Guagliardo et al., 2022). In response to COVID-19 outbreaks related to maritime transport, diverse reactions were observed with reports of cruise ships denied port entry and travellers unable to disembark; starting in March 2020 the extraordinary suspension of cruise ship travel by cruise line operators was seen as a means to mitigate the spread of COVID-19 (CLIA, 2020).

Moreover, cruise ships were reported as being responsible for super-spreading events (Abe et al., 2022; Althouse et al., 2020; Frieden et al., 2020). There is now sufficient evidence that the pathogen responsible for COVID-19 is transmitted primarily through exhaled aerosol particles suspended in indoor air (Tang et al., 2020; Wang et al., 2021). It is clear that aerosol generating activities (e.g., breathing, talking, eating, singing), physical proximity and ventilation conditions determine transmission (Jayaweera et al., 2020; Morawska et al., 2020), and that the risk of infection to airborne respiratory disease increases when people share an enclosed and poorly ventilated space (Setti et al., 2020). Marine aerosols are composed of sodium chloride, other inorganic salts, atmospheric particles and organic matter and are primarily formed through the burst of rising bubbles on the sea surface or waves breaking (Aller et al., 2005; Sun et al., 2024). The transport of bacteria and viruses from the sea to the atmosphere mainly occurs through this aerosol formation and the sea-surface microlayer may be the most important source of these microorganisms (Aller et al., 2005). Although the high humidity could be a relevant point in decreasing virus spread (Bozic et al., 2021), the semi-enclosed high occupancy environment aboard cruise ships is a relevant factor for the spread of infectious diseases.

Hotel load, or ship's non-propulsion-related power demand, typically constitutes approximately half of the cruise ship's total energy consumption including components such as lighting, auxiliary machines, navigation, refrigeration, and heating, ventilation and air conditioning (HVAC). HVAC systems consume up to 40% of the total hotel load (Aarnio, 2022; Brækken, 2023). A large passenger cruise ship is generally equipped with numerous air handling units (AHUs), taking up a large proportion of the ship's interior space. AHUs condition the air to a desired supply air temperature and RH. The operation of such an HVAC system is extremely energy-consuming (Aarnio, 2022), especially in hot and humid climates, where supply air dehumidification significantly adds to the energy use (Wang, 2024). Therefore, various solutions have been exploited to reduce energy consumption. Researchers have suggested several such solutions including partial air recirculation, demand-controlled ventilation system (DCV), thermal energy storage, heat pumps, solar energy and heat/moisture recovery (Aarnio, 2022; Brækken, 2023). Among these solutions, air recirculation and heat recovery are the most commonly implemented (Kosako and Shiiyama, 2008; Mihai and Rusu, 2021). While partial air recirculation significantly reduces energy consumption by decreasing the amount of outdoor air delivered, this typically results in lower indoor air quality (IAQ) and can consequently increase infection transmission risk (Almilaji, 2021; Mihai and Rusu, 2021; Xu et al., 2020). Following the COVID-19 pandemic, professional institutions have proposed new ventilation standards (Section 2.6), mainly emphasising a change for a regular supply of 100% outdoor air. Ren et al. (2022) evaluated the impact of various ventilation strategies on disease infection risk in an office environment. The findings indicated that ventilation approaches with less recirculation effect in the room (zone and stratum ventilation) could potentially decrease infection probabilities to approximately 19%.

There have been several studies that have explored the correlation between CO₂ concentrations, exhaled breath and the risk of exposure to airborne diseases in indoor spaces. A list of recent

publications, summarised in Table S1, shows a focus on monitoring CO₂ levels to either: (i) investigate the risk of COVID-19 infection transmission in mass-gathering indoor spaces; or (ii) explore IAQ or disease transmission risk on board passenger ships. This summary of existing research articles (Table S1) indicates numerous research gaps on this topic. Firstly, monitoring studies have mainly been focused on educational institutions (Adzic et al., 2022a; Fantozzi et al., 2022; Muelas et al., 2022; Park and Song, 2023; Villanueva et al., 2021; Schibuola and Tambani, 2020); stadiums and concert halls (Adzic et al., 2022b; Malki-Epshtein et al., 2022; Schade et al., 2021); office and residential buildings (Yin et al., 2022; Bazant et al., 2021), supermarkets (Li and Tang, 2022); hospitals (Crews et al., 2024; Kumar et al., 2022) and restaurants (Kumar et al., 2022; Park and Song, 2023). Secondly, there is also a noticeable deficiency in comprehensive data collection for infectious disease transmission risk specific to the human transportation sector. Monitoring-based experiments and computational fluid dynamics (CFD) modelling have been conducted around different modes of transportation, including trains (Schmeling et al., 2022; Woodward et al., 2021; Wang et al., 2022), buses (Edwards et al., 2021; Malki-Epshtein et al., 2020) and planes (Yan et al., 2017; Zhang et al., 2021; Wang et al., 2021). However, there are limited studies investigating ventilation conditions on board passenger ships (Kim and Lee, 2010), and research on the effectiveness of ventilation provision for passenger ships in disease mitigation is relatively scarce (Kumar et al., 2024). The unique environmental conditions of passenger ships are characterised by their semi-enclosed and densely occupied spaces where travellers from different origins may interact for prolonged time periods. Unlike typical residential or commercial environments, passenger ships, especially cruise ships, integrate living, working, entertainment/social and dining areas in a compact layout, necessitating specialised IAQ studies and research on the probability of infectious disease for passengers and crew over the duration of their voyages.

The World Health Organisation (WHO) declared an end to the public health emergency of international concern in May 2023 (WHO, 2023) and the post-COVID-19 recovery is well underway. The cruise sector is expected to experience an unprecedented rebound to achieve even higher passenger volumes than prior to the pandemic, in particular the first summer holiday season since COVID-19 restrictions have eased globally. Major viral disease outbreaks that emerged over the past decades have mostly involved airborne respiratory viruses, including SARS CoV-1, Middle Eastern Respiratory Syndrome (MERS), SARS CoV-2 (Bhadoria et al., 2021) and H1N1 influenza Pandemic (2009). Given the high contagiousness of COVID-19 and airborne transmission of the disease, crowded and enclosed gatherings can create environments conducive to aerosol virus transmission with a reduction in physical distancing behaviour (Zhu et al., 2023). The authors recognise the limitations of control measures and the challenges in the effective detection of cases currently in place on board cruise ships. There might be a risk that ventilation provisions are only able to provide adequate IAQ and thermal comfort, but are not sufficient for disease mitigation in semi-enclosed high occupancy environments aboard.

The European Union (EU) project HEALTHY SAILING funded under the Horizon Europe Framework Programme has undertaken a task to understand the ventilation conditions, dispersion mechanism and the risk of airborne disease transmission in a mass-gathering passenger cruise ship, while providing a reliable data set that could be used to validate CFD models of aerosol dispersion. For the first time, in the framework of this project, monitoring of CO₂ (as a proxy of ventilation and for exposure to exhaled breath) and thermal comfort parameters (temperature and RH) was conducted in different environments on board a sailing cruise ship voyaging across the UK and Europe. Indoor CO₂ accumulates from human metabolism (Peng and Jimenez, 2021) and exhaled air may contain pathogen-laden aerosols (Adzic et al., 2022). The measurements of indoor CO₂ concentrations can often be an effective indicator of occupancy relative to the level of ventilation, which links to the risk of aerosol

transmission indoors (EMG and SPI-B, 2021). The localised monitoring of CO₂ can provide spatially and temporally resolved data, to identify the effectiveness of ventilation (e.g., high concentrations of CO₂ indicate low levels of ventilation and/or high occupancy) and the impact of occupancy distribution and space volume on IAQ. Thus, this paper has exploited CO₂ concentrations as a practical proxy for airborne transmitted diseases and ventilation, as pathogen-containing aerosols and CO₂ are co-exhaled by infected persons (Peng and Jimenez, 2021).

The overall goal of this work is to build an understanding of the ability and agility to mitigate the risk of virus transmission on board a large passenger ship, thus providing a healthy sailing environment for crew members and passengers whilst the industry returns to full normality in the post-COVID-19 era. The specific aims are to: (i) assess the ventilation conditions on a sailing cruise ship, (ii) identify the potential role of ventilation-related measures to reduce the risk of airborne virus transmission, (iii) explore the potential of energy-saving, based on the IAQ and probability of infectious risk obtained, and (iv) provide a real-world dataset to allow for an IAQ classification.

2. Methodology

2.1 Site description

The study was carried out on a passenger cruise ship carrying over 5000 passengers, sailing, manoeuvring and porting in the UK and the EU in August 2023 (name of the cruise ship has been anonymised for confidentiality purposes). The monitored locations comprised nine indoor spaces aboard, including (1) buffet, (2) gym, (3) bar, (4) restaurant, (5) pub, (6) theatre, (7) standard double occupancy cabin with male occupants, (8) standard double occupancy cabin with female occupants, and (9) standard double occupancy cabin with a single male occupant. Table 1 summarises monitoring dates and duration, to maintain anonymity,

these indoor spaces are referred to by their generic names. Table 2 briefly summarises each monitored location's characteristics, including its maximum occupancy and floor area. The maximum occupancy is assumed based on the number of seats available in each venue, and therefore on some occasions, there may be additional occupancy. For example, in the pub and bar, during peak hours when the seats are fully occupied, additional people could potentially be standing. It should be noted that occupancy for the Gym is an estimation based on physical observation, as there is no specific seating in this venue. Additionally, Figure S1 presents engineering schematic drawings showing the experimental layout of monitoring locations and the position of CO₂ sensors. Due to the logistics and health and safety requirements on board a large passenger ship, air quality monitoring in public spaces under supervised conditions is not feasible. As such, data were collected unsupervised daily on a 24-hour basis. Regular physical and remote checks (sensors' mobile app) were performed every two to three hours to make sure sensors were working properly. Table S2 describes the typical operating hours for the monitored locations.

2.2 Location characteristics

The vessel is equipped with DCV systems that include CO₂ and temperature sensors in part of the locations aboard to maintain a fixed internal temperature of 22.5 °C, meaning the ventilation is variable depending on the occupancy. The characteristics of each of the nine monitoring locations are given below.

- **Buffet:** Located on deck 15, this monitored location encompasses only one-third of the total indoor area of the buffet (refer to Figure S1). This place has an open kitchen and spans approximately 1217 m², accommodating up to 306 guests. The opening hours were 06:30-02:00 and consisted of four serving sessions: breakfast (06:30-11:30), lunch

(12:00-16:00), dinner (18:00-21:00) and midnight (22:00-02:00). The CO₂ sensor was positioned near the centre of the room and collected 171.25 h of data.

- **Gym:** Located on deck 16, this area has an estimated maximum occupancy of 50 people and spans an area of 570 m². The gym consisted of a compact fitness area equipped for indoor workouts including equipment such as treadmills, weight training benches, stationary bikes, and dumbbells, among others. The gym opening hours were 06:00-22:00. The CO₂ sensor was positioned on top of a shelf and monitored for 166.5 h.
- **Bar:** Situated on deck 18, this area consisted of a piano lounge and a bar, featuring bistro tables and a floor-to-ceiling window offering a panoramic view with live band performances during evening hours. With a maximum occupancy of 180 people and covering an area of 630 m², the bar was opened 10:00-01:30 on sea days and 16:00-01:30 on port days. The CO₂ sensor was installed atop a lamp near the piano in the main section of the bar and monitored for 166.45 h.
- **Restaurant:** Situated on deck 5, this was one of the main restaurants with an open space of 1050 m² and a maximum occupancy of 598 people. The restaurant required advance booking and was only open during dinner hours, with three available time slots: 17:30, 19:30, and 21:30. The CO₂ sensor was mounted within a wooden frame near the room's centre and monitored for 165.55 h.
- **Pub:** Located on deck 7, this area embodies the ambience of a traditional English pub, covering 200 m² with a maximum occupancy of 81 people and featuring a few large TV monitors for live sports games. Opening hours were 11:00-02:00. The CO₂ sensor was positioned atop a pillar near the ceiling and monitored for 100 h.
- **Theatre:** Located across two levels on decks 5 and 6, the theatre is a large open space with 1000 m² that features a raked floor design and accommodates various events such as theatrical performances and shows. Daily presentations are scheduled during the

evening at 19:00, 20:30, and 21:45 (matinees/afternoon shows only occur on sea day), with a maximum occupancy of 945 people. The CO₂ sensor was fixed near the entrance of the venue, situated on the prompt desk controlling the visual and acoustic effects of the performances and monitored for 99.25 h.

- **Cabin M (male cabin) and Cabin F (female cabin):** Both cabins were situated on deck 13, featuring a floor area of 17 and 10 m², respectively. They were reserved for the research team and accommodated two occupants each at the time of monitoring. Each cabin comprised a compact double room with amenities including a wardrobe, double bed, bedside tables, vanity area with a small table, and an attached bathroom separated by a door. Occupancy patterns varied but primarily occurred during the morning and early afternoon hours. AC rates differed between the rooms, based on settings adjusted by the occupants. The CO₂ sensor was placed on top of a table and monitored for approximately 126 h.
- **Cabin S (single occupant cabin):** This cabin was a standard double occupancy sized cabin with the same features as the above cabins, but only had a single occupant during the time of monitoring. It is located on deck 11 and encompasses a floor area of 17 m². The occupancy times are similar to the above cabins as the research team worked together and followed the same schedule of activities. The CO₂ sensor was left on top of a table and measured for 80.75 h.

2.3 Instrumentation

The CO₂ concentrations were determined using HOBO MX CO₂ logger model MX1102 (Onset Computer Corporation); referred to hereinafter as HOBO, which uses non-dispersive infrared (NDIR) spectroscopy to measure CO₂ concentrations in a non-condensing environment. The sensor features an auto-calibration and can measure CO₂ concentration across a range of 0-5000 ppm, with a 1 ppm display resolution, and accuracy of ± 50 ppm or

±5% of the reading (whichever is higher) at a temperature of 25°C, RH below 70% and pressure of 1013 mbar (HOBO, 2015). These sensors were installed in each location at a sitting/breathing height of ~1 m whenever feasible, or at a higher position for safety purposes (to avoid the reach of children). Figure S2 provides an example of the instrument setup. The sensor is fitted with a data logger that records data at an interval from 1 s to 18 h. In the current study, data were recorded every 60 s. Moreover, each instrument has an integrated sensor that records and transmits temperature and RH data at the monitored locations. The HOBO sensor can measure up to 6 months with the same battery and should be used in indoor environments and not be exposed to extreme RH and temperatures. Therefore, the locations selected to allocate the sensor were exclusively indoor environments.

Data quality control and assurance procedures were conducted, which included the co-location of HOBO sensors with Q-Trak IAQ monitor Model 7575 (TSI Incorporated), referred to hereinafter as Q-Trak. The co-location procedure involved the HOBO sensors and two factory-calibrated Q-Trak and is discussed in detail in Section 2.8. Q-track uses a non-dispersive infrared (NDIR) sensor to measure CO₂, as well as a thermistor to measure temperature and a thin-film capacitor to measure RH. It can measure CO₂ across a range of 0-5000 ppm, with a 1 ppm resolution. The accuracy is ±50 ppm or ±3% of the reading, whichever is higher. The indicated instrument operating conditions include an altitude of up to 4000 m and a RH of up to 80% (Q-TRAK, 2016).

2.4 Data collection and analysis

CO₂ concentrations, temperature and RH data were sampled continuously from the unattended and unsupervised monitoring sites, throughout the cruise voyage. The deployments of instrumentation are split up into three phases: buffet, restaurant, gym, and bar in Phase 1 (started on 16.08.2023), cabin M, cabin F, theatre, and pub in Phase 2 (started on 19.08.2023)

and finally cabin S in Phase 3 (started on the 20.08.2023). This was due to complex logistics in obtaining permission to access and undertake monitoring activities in the mass-gathering locations aboard. The temperature, RH and CO₂ data were acquired using the mobile software HOBOnnect^R by ONSET for IOS, version 1.6.1. The obtained data were retrieved as a .csv file from the software, and then analysed using several software, including Microsoft Excel Version 2311 by Microsoft Corporation (Redmond, Washington, USA), Google Colaboratory by Alphabet Inc. (Googleplex, California, USA) and Python Data Analysis Library - Pandas 1.5.3 via NumFOCUS, Inc. (Austin, Texas, USA).

2.5 Estimation of ACH and VR

ACH was calculated using CO₂ concentration data that took into account both occupancy and subsequent CO₂ levels, while ACH here refers to the total outdoor air coming into the space. We applied the decay method for calculating the ACH in these nine locations on board the cruise ship, following the methods used by prior studies (Abhijith et al., 2022; Canha et al., 2013; Kumar et al., 2022; Kumar et al., 2024). The decay of CO₂ was calculated by evaluating the CO₂ concentration until it reached approximately 420 ppm, which is regarded as the background level (GML, 2024), when the occupants had vacated the venue. A random peak has been selected for the calculation of the pub, buffet, gym, bar and cabins, due to a constraint related to the operating hours of these locations (operating continuously until late at night) and the unknown occupancy in the spaces. It is therefore extremely challenging to observe a full decay cycle for the ACH calculations. Conversely, because of the scheduled operating hours for the restaurant (three dinner serving periods during the evening) and the theatre (two afternoon and three-night shows), the decay of CO₂ was calculated around their closing hours when occupants left the venue. Finally, the daily values of ACH and VR were calculated for each monitoring day and the averages were taken.

311 The ACH obtained by the decay method (AD) was calculated through Equation (1):

312
$$AD = 1 / \Delta t \ln[(C1 - CR) / (C0 - CR)] \quad (1)$$

313 where Δt is the time (h) between C0 and C1, C0 is the CO₂ concentration obtained at the
314 beginning of the sampling period (ppm), C1 is the CO₂ concentration at the end of the sampling
315 period (ppm), and CR refers to the lowest CO₂ concentration in the make-up air or the steady-
316 state concentration at the lower occupancy (ppm).

317 CO₂ is inherently produced by human activities and co-exhaled by the venue occupants. The
318 exhaled CO₂ is then diluted by the ship's ventilation system. The ventilation rate was estimated
319 using the CO₂ component balance (Hama et al., 2023), which considered the below premises:
320 (i) the ship's indoor space is well mixed, (ii) the occupants are the only source of CO₂, except
321 as otherwise specified, (iii) each occupant breath at a steady rate and exhale constant CO₂
322 concentration, (iv) CO₂ above a standard background ambient concentration of 420 ppm in the
323 indoor environment is the result of exhalation of the occupant(s) in that space, and (v) ACH
324 and VR were constant throughout the day. The following criteria were used for each decay
325 sequence: (1) C1 should be relatively close to the background CO₂ concentration of 420 ppm;
326 (2) the Δ CO₂ (difference in concentration between C0 and C1) must exceed 100 ppm or should
327 be greater than the standard instrument accuracy.

328 The VR at design/assumed occupancy in m³ h⁻¹ was obtained by multiplying the ACH with the
329 volume (V, m³) of the monitored locations and dividing it by the number of maximum
330 occupants of each location, using Equation (2).

331
$$VR = ACH \times V \times person^{-1} \quad (2)$$

2.6 Guidelines for evaluating IAQ, ventilation condition and thermal comfort

The main guidelines concerning indoor environmental quality typically followed in the UK were introduced by the Chartered Institution of Building Services Engineers (CIBSE), American Society of Heating, Refrigerating and Air-Conditioning Engineers (ASHRAE), Federation of European Heating, Ventilation and Air Conditioning Associations (REHVA), Scientific Advisory Group for Emergencies (SAGE) and Health and Safety Executive (HSE). Table 3 shows the recommended targets suggested for the evaluation of CO₂, VR, temperature and RH.

The HVAC systems are intended to maintain sufficient thermal comfort and IAQ on board. The international standard “ISO 7547:2022: *Ships and marine technology – Air-conditioning and ventilation of accommodation spaces and other enclosed compartments on board ships – Design conditions and basis of calculations*” (ISO, 2022), has defined the design conditions for summer and winter conditions (Table S3). Furthermore, the standard states that the minimum outdoor air supply shall not be less than 0.008 m³ s⁻¹ person⁻¹. The British standard “BS EN 16798 - Energy performance of buildings. Ventilation for buildings” (Table S5; BSI, 2019), has defined IAQ acceptance in four bands based on occupant comfort and expectations. A high acceptance level (band 1) indicates good IAQ that is advised to operate for vulnerable groups of occupants. Conversely, a lower acceptance level (band 4) will not pose immediate health risks but may decrease occupants’ comfort and satisfaction.

2.7 Infectious risk evaluation

The potential risk of airborne disease transmission for SARS-CoV-2 was estimated by employing a well-mixed Wells-Riley model (WRM), which has been adopted by numerous previous studies (Buonanno et al., 2020a, 2020b; Fantozzi et al., 2022; Kumar et al., 2022; Woodward et al., 2022). Several assumptions are made including (i) no viruses are present at

the beginning of the analysis, (ii) the viral load increases throughout the analysed period, (iii) the number of source infectors is equal to one (Dai and Zhao, 2020) and (iv) infected and susceptible occupant always resides in the space over the entire duration of the analysis. The calculation is based on the notion that the air contains doses of the infectious virions, and that occupants will become infected by breathing a single dose. The infected person breathes out virus-laden particles at a constant rate, and the infectious dose of the virus can be removed when it decays, falls onto a surface or is diluted by ventilation. The infection probability estimation using the WRM is given by Equation (3; Sze To and Chao, 2010).

$$p_i = 1 - \exp\left(-\left(\frac{r_{DOUT} B t_R}{V_R(1/\tau_D + 1/\tau_F + 1/\tau_{VF})}\right)\right) \quad (3)$$

where r_{DOUT} is the virus emission rates from the infected person, B is pulmonary ventilation rate ($0.8 \text{ m}^3 \text{ h}^{-1}$; Miller et al., 2021), t_R is the exposure time (h); τ_D is the time constant for viral inactivation (0.32 h^{-1}), τ_{VF} is the ventilation rate (h^{-1}), τ_F is the deposition rate (0.3 h^{-1}), and V_R is the volume of the indoor environment (m^3). The accurate volume of the indoor environment is provided by the cruise company (Table 2) and the ventilation rate in ACH (τ_{VF}) is estimated with occupancy and CO_2 concentration monitored (Section 3.4).

2.8 Quality control and assurance

The instruments used in this study have been frequently used in many IAQ studies (Coulby et al., 2021; Deng and Lau, 2019; Kumar et al., 2022; Kumar et al., 2023). The monitors underwent co-locations with a factory-calibrated instrument and subsequent correction factors were calculated and applied to the data. Additionally, prior to the deployment, the CO_2 monitors were manually calibrated at 400 ppm in ambient conditions as directed by the manufacturer using their auto-calibration feature. This allowed the monitors to have satisfactory accuracy during the sampling period. CO_2 concentration values below 350

ppm were removed from the data as outliers, since it is expected that the average daily outdoor CO₂ levels vary around 300 ppm and values below that would not be realistic.

The HOBO sensors were co-located with Q-Trak monitoring sensors in a university office space (Figure S3) before and after the monitoring campaign. Human exhaled breath was used as the source for the generation of CO₂ concentration. The instruments were placed closely together on a table inside an office space (with the supply air inlet at a reasonable distance) and to be left operating and monitoring for approximately 8 h, while the occupants continued working as usual. During the experiment around 6 people were present. With this procedure, a linear regression factor and error estimate were obtained for CO₂ concentration for each HOBO at a frequency of 60 s. Initially, the instruments were turned on and left to warm up for at least 30 minutes. During this time the sensors were acclimatising to the room conditions and also sampling a background concentration for the room. After this time, the actual experiment started, and the equipment was left running for at least 7 h. During the experiment, opening the windows and the amount of people inside the office were used to vary the CO₂ concentration. Therefore, when the concentration was too high the windows would be opened accordingly. Vice-versa, for some situations when people left the room, and the concentration began to decrease, either the windows would be closed, or occupants would be asked to return. This procedure allowed the comparison of various concentration ranges between the calibrated Q-Trak and HOBO sensors. After this procedure, the data obtained were analysed. Results and data obtained from the co-location experiment are shown in Figure S4. The factory-calibrated Q-Trak has a strong and positive correlation with the Hobo CO₂ sensors, correction factors are calculated (Table S4) and the results show that the adjustments required are minor. However, most HOBO monitors reported lower average CO₂ concentrations than the referencing sensor Q-track during the colocation studies. This indicates that instruments with the same make/brand and sensing principles might have minor differences in sensitivity to CO₂. Therefore, a linear

regression model was developed and correction factors were applied to the dataset to optimise the comparability of measurements between different monitored environments (Table S4).

3. Results and Discussion

This section elucidates the data obtained from the monitoring aboard, including: (i) typical concentration of CO₂, temperature and RH on board a large cruise ship and their correlation; (ii) discussing variation of CO₂, temperature and RH caused by occupancy, venue design characteristics, ship operational behaviour (voyaging and berthing) and HVAC operation mode; and (iii) investigating ventilation performance and infectious disease transmission risk based on ventilation provisions.

3.1 CO₂ concentration in different microenvironments

Figure 1 shows a time series of the CO₂ concentrations for all the monitored locations. Figure S5 shows a combined hourly average plot. Given the variation in CO₂ concentration within the monitored compartments (Figure 1), clearly, the cruise ship environment as a whole cannot be considered to be well mixed. This is due to a number of factors such as the differences in mechanical ventilation conditions, natural ventilation conditions and occupancies. All figures show event start (beginning of sensor deployment) and event end times, with data presented at one-minute intervals. The blue highlighted sections represent the days when the cruise ship was sailing (sea day, 21.08.2023 and 23.08.2023). The results show that the second sea day (23.08.23) presented higher CO₂ concentrations compared to the first sea day (21.08.23) in the buffet, restaurant and theatre.

The results also denote that each monitored site exhibits repeatable trends with peaks occurring each day approximately at the same time. This is to be expected as passengers follow a routine pattern of behaviour each day. Therefore, the data obtained could be an effective indicator for

identifying the typical peak periods for different venues or locations on board the cruise ship, which could be then utilised for improving ventilation strategies. The evidence that the ship has observable peak hours, with varying ventilation performance (CO₂) in mirror environments implies that occupancy has a significant impact on CO₂ distribution and there may be insufficient ventilation for the actual occupancy. Estimated typical peak hours for some of the locations can be observed from the data (Figure 1). The pub typically has a steadily rising trend from 18:00 onwards, reaching its peak at around 21:30-22:00. Two peaks (morning and night) were identified for the buffet during the day, with the breakfast peak starting from 09:00-11:00 and the dinner peak at around 21:00. The restaurant data shows two peaks, the morning peak starts from 10:00-11:00 and the evening peak begins from 18:00-21:00. The bar is typically busiest after 19:00, and usually reaches its peak at 21:00. The gym concentrations usually peak before dinner at around 18:00. Additionally, it can be noted from the data that CO₂ levels in the three monitored cabins follow similar peaks and troughs. The variation in CO₂ concentrations could be considered a coincidence here because these cabins were allocated to the research team, so they would typically follow the same schedule of activities as they were working together. For instance, the majority of the peaks occur in the morning to afternoon period, as the research team worked during the night.

Figure 2 shows the box plot for CO₂ concentrations, temperature and RH at all monitored locations. The CO₂ concentrations boxplot (Figure 2a) shows that most of the venues have a strong positive skew and the theatre, restaurant, and pub have several extreme outliers. Among these, the restaurants have the largest outlier value, with over 2500 ppm, followed by the pub with over 2000 ppm. The interquartile ranges (IQR) of cabin M and cabin F are similar; this corresponds to the similar occupancy times due to the almost identical work patterns of the research team. Overall, the theatre, bar, gym and buffet have less dispersed data and the median CO₂ concentration of the theatre, pub, and bar is under 500 ppm which is lower than other

monitored sites. The mean CO₂ concentrations in the theatre are relatively lower, indicating it is either mostly unoccupied and/or has excellent ventilation performances. Locations with a large number of outliers show a bimodal pattern, which can be inferred that spaces are not used most of the time. Therefore, some data during the peak occupancy have been labelled as outliers. As a consequence, the mean/median concentrations are low. Thus, data from the active hours at each venue have been extracted and outlined in Figure S6. Results show a less positive skew distribution, particularly for the theatre, restaurant and pub, with a significant increase in the mean/median concentrations.

The temperature boxplot (Figure 2b) shows the distribution of the temperature data. Results indicate that entertainment areas, including the theatre and gym, have the least dispersed temperature data. While dining areas, including buffet, restaurant and pub, have overall more scattered data, the pub recorded the lowest median followed by the restaurant. For cabin M and the bar, data appeared to be negatively skewed, while the buffet showed positive skewing, with the rest of the locations showing relatively symmetric data. The IQR temperature of cabin M is the highest and cabin F has the largest range of outliers. The range of temperature aboard was recorded at 22.3 ± 1.4 °C (mean \pm standard deviation) across nine monitored locations). The distribution of the RH data (Figure 2c) indicates that the medians of RH for all monitored locations are around 70%. The median of cabin M is the lowest at under 60%, while the restaurant has the highest median of around 73%. The data for cabin F, cabin S and theatre are negatively skewed, and the data for the pub, gym and buffet are positively skewed, with the rest of the box plots being symmetric. Overall, the range of RH across the nine monitored locations was $68.2 \pm 5.3\%$ (mean \pm standard deviation).

3.1.1 Air quality classification

To obtain a comprehensive picture of the IAQ for the shipboard environment, the ventilation performance was determined for each monitored location and then aggregated. To identify the worst performance for each space, the maximum CO₂ values (the outliers presented in the box plot) obtained were found (Figure 2a). The spaces were then classified into air quality bands following the targeted standard defined by British standard BS EN 16798 (Table S5; BSI, 2019). The average air quality was in band 2 (medium acceptance level) for ~75% of the monitored sites. A considerable number of spaces were in band 3 (moderate acceptance level), which is equivalent to a CO₂ concentration exceeding 1750 ppm. Classification based on maximum CO₂ (outliers) suggested that the general IAQ on the cruise ship is highly acceptable for the majority of the time.

Locations with excellent and highly acceptable IAQ include Cabin S (classified in band 1), the bar and the gym, with maximum CO₂ concentrations at 942 ppm, 1062 ppm and 1072 ppm, respectively. Cabin M and cabin F are classified in band 2 (medium IAQ acceptance) with maximum CO₂ levels of 1147 ppm and 1255 ppm, respectively. The theatre is also classified in band 2 with maximum CO₂ concentrations recorded at 1721 ppm, however, only short-lived peaks can be observed for the theatre (Figure 1), which indicates that the occupancy plays an important contribution to the elevation of CO₂ concentration. Although cooking activities occurring in the buffet may have affected the overall IAQ beyond CO₂, the maximum CO₂ concentration recorded is just slightly over 1000 ppm standing at 1102 ppm. This might be attributed to the fact that the buffet is located on deck 15 with a large outdoor dining area, separated from the indoor buffet by automatic doors that will open whenever guests enter, allowing outdoor air to infiltrate and dilute the CO₂ concentration.

The pub and the restaurant have the highest maximum CO₂ concentrations, hence the worst IAQ classification; both locations are classified in band 4 with 2109 ppm (113 minutes above 1750 ppm) and 2787 ppm (171 minutes above 1750 ppm) respectively. This means occupants can exhibit symptoms such as drowsiness, difficulty concentrating, and be exposed to infectious disease risk (Satish et al., 2012), thus these spaces are a priority for improvement. A fairly patterned peak sequence can be observed in the pub during the evening, mostly exceeding 1500 ppm. Similarly, the restaurant generally exceeds 1200 ppm during the dinner period, and CO₂ concentration in the restaurant on 23.08.2023 showed a significant spike of up to 2787 ppm. This result could be due to the higher footfall of the pub and restaurant, 0.6 person/m⁻² and 0.4 person/m⁻², respectively. Because personal protective equipment (PPE) cannot be used while eating and drinking, these locations should be prioritised for improvement. In addition, celebration parties and additional performance activities by crew members on 23.08.2023, the last day before disembarkation in the UK, could explain the elevated CO₂ concentration in the buffet, restaurant and theatre.

3.2 Variations in indoor temperature and RH

A thermally comfortable indoor environment is crucial for the occupant's health and productivity (Kaushik et al., 2020). The ASHRAE “Thermal Environmental Conditions for Human Occupancy” guidelines (2013) have defined a satisfactory thermal condition for a typical occupied building space, a standard of 21-23°C in the winter and 22-26.5°C in the summer. Both indoor air temperature and RH are crucial contributors to airborne transmission and infectivity of infectious disease particles (Aganovic et al., 2021; Guo et al., 2021; Mao et al., 2023). The thermal conditions could affect evaporation conditions, and consequently pose changes in the constituents of virus particles negatively affecting the virus' survivability (Noti et al., 2013). Thermal sensation or exposure to high temperatures could also influence human immune response and infection susceptibility (Nottmeyer et al., 2023; Kumar, et al., 2022).

Figure 3 shows a time series plot for temperature and RH to understand the thermal condition. The data indicates that the relationship between RH and temperature in a shipboard environment behaved in its normal inversely proportional relationship; an increase in temperature would lead to a decrease in RH and vice-versa. However, the pub provided an exception demonstrating very similar trends for temperature and relative humidity. The initial hypothesis for the unusual correlation is that the crowded environment and activities undertaken by pub occupants (pouring beer, drinking alcohol and speaking loudly) caused an increased human body temperature or excessive moisture generation. Considering the summer temperature thermal sensation guideline, the results (range of temperature: $22.3 \pm 1.4^{\circ}\text{C}$) suggested that the cruise ship thermal sensation aboard was found to be generally excellent, while most locations were occasionally found to be over-air-conditioned, especially the cabins and gym, with relatively lower internal temperatures of $20\text{-}21^{\circ}\text{C}$. In contrast, dining areas have experienced higher air temperature, potentially due to human behaviour (eating and drinking) and social activities conducted in the venue have exhibited an increase in human body temperature (Perry et al., 2020) or the heat generated from the kitchen nearby.

In addition, when considering typical ship ventilation design conditions, ISO 7547 (2022) applies (Table S3), which adopts seasonal recommendations for onboard thermal sensation characteristics. It is suggested during the summer season, the temperatures and humidity for indoor air aboard be 25°C and 55%, respectively. The data in Figure 3 shows that throughout the monitoring period, all monitored locations have mostly recorded RH above 55%. Conversely, most of the monitored locations (except the bar and cabin M) have temperatures below 25°C .

Air temperature and RH influence the spread of airborne infectious disease, as relatively warmer ($25\text{-}30^{\circ}\text{C}$) and wetter climates seem to reduce the risk of spread (Nottmeyer et al.,

2023; Mecenas et al., 2020). Studies (Aganovic et al., 2021; Guo et al., 2021; Noti et al., 2013; Verheyen and Bourouiba, 2022) have reported that intermediate indoor RH (40-60%) is found to provide sufficient satisfaction in the thermal environment and reduce the efficient of microbial growth, viral survival and infectivity. As discussed in Section 3.1, the range of RH aboard was $68.2 \pm 5.3\%$, while dining areas and gym were averaging in the higher quartiles of the RH region of 75-80%. Although, debate exists over how RH directly affects the transmission and viability of viral disease. It is recommended that humidity control be implemented for the prevention of dust mites and mould growth; which can negatively affect respiratory health by triggering allergic responses (Jones et al., 2022).

3.2.1 Correlation between CO₂, temperature and RH

Research has shown a possible influence of air temperature on CO₂ emissions by occupants indoors (Angelova et al., 2022; Fang et al., 1998). However, since a plausible mechanism explaining this link is not currently available, it is inappropriate to assume a direct relationship between them. For example, it is possible that the correlation may be caused by a third factor such as the building design, or the presence of multiple occupants in a room which could increase indoor CO₂ concentration. This section aims to explore the dispersion of CO₂ and the potential influence of temperature and RH on CO₂ emissions by occupants in shipboard environments.

Figure 4 shows CO₂ concentration versus thermal comfort parameters on a sea day (21.08.2023) during peak hours from 16:00-23:00. This period was selected as occupants play an important role in the variation of CO₂ concentration and peak hours/occupancy could more realistically account for the observed correlation. The absolute CO₂ concentrations (CO₂ levels before applying correction factors) were used for the plots in this section, to avoid a bias of data and enable a direct comparison of actual CO₂ concentrations against thermal parameters

in each separate venue. Figure 4a shows CO₂ concentration versus temperature, indicating that the pub and theatre have strong positive relationships, while the bar has a negative relationship. Figure 4b shows CO₂ concentration versus RH, indicating that the pub, bar, gym and restaurant have strong positive relationships, while the buffet has a weak negative relationship, and the theatre has a strong negative relationship. The cabins are not considered for this discussion since the thermostat could be individually adjusted by occupants, however, Figure S7 shows the scatter plots for the three cabins.

Furthermore, results indicate that temperature and RH can be good indicators of higher occupancy. The higher temperature is usually related to an elevated CO₂ concentration, except for the bar, with an inverse correlation between CO₂ and the temperature (lower temperature relates to higher CO₂ level), which could be due to the direct sunlight exposure from the full floor-to-ceiling glass feature of the bar, causing an internal temperature increase. Contrarily, a lower RH is usually related to an elevated CO₂ concentration, except for dining areas including the pub, restaurant and bar. While the inverse correlation phenomenon for the bar and pub can be explained by temperature and RH behaved in their normal inversely proportional relationship, and excessive moisture generation by pouring beer, respectively (Section 3.2). However, the direct influence of indoor temperature and RH on CO₂ exhalation by occupants will require further exploration.

3.3 Impact of venue characteristics and operational behaviour

3.3.1 Density frequency distribution

The kernel density distribution plots in Figure 5 help to understand CO₂ concentration and temperature peak frequencies and their spread. These density plots are a smoothed form of histograms that depict the distribution of data using the density function to estimate a continuous curve. The monitored sites are also grouped into sub-categories based on different

design conditions, including the deck ceiling height (Figure 5d) and the volume of the venue (Figure 5e). The averaged CO₂ concentrations are plotted for each of these subgroups to understand the impact of these design characteristics on the CO₂ concentrations. Additional density plots of the averaged CO₂ concentrations (Figure 5a), temperature (Figure 5b) and RH (Figure 5c) are plotted to illustrate the occurrence of the range of CO₂ concentrations, temperature and RH. The subgroups defined for Figures 5d and 5e are outlined in Table S6.

Figure 5a shows the density plot of CO₂ concentration for different ship microenvironments. The distributions exhibit bimodal features for most of the monitored locations, with variable peak heights and widths across different ranges. For instance, the cabins, gym, bar and buffet showed a narrower peak CO₂ concentration between 400 and 800 ppm, while the restaurant and pub showed an elongated tail on the right side of the density plot, illustrating a low frequency across the higher CO₂ concentration range. Figure 5b illustrates the distributions of indoor air temperature for different ship microenvironments. These showed unimodal distribution for all monitored locations, except the restaurant. For instance, the peak density of the gym is the highest and sharpest (range from 20.5-22.5°C), which is an indicator of a less frequent occurrence of higher indoor air temperature. Dining areas (pub, buffet, restaurant and bar) typically have a short and broad peak distribution, diminishing in a wide range between 19.5-25.5°C, indicating that the variation of occupancy level heavily influenced indoor temperature. Figure 5c illustrates the distributions of RH for different ship microenvironments. As discussed earlier, because RH and temperature behaved in its normal inversely proportional relationship, therefore similar to Figure 5b, unimodal distribution can be observed for most monitored locations, except restaurant. While majority of the locations have peak frequencies of RH occurring in the range of 65-75%. Figure 5d shows the density plot of CO₂ concentration for different ceiling heights of indoor spaces aboard and the density distribution plots showed an unimodal distribution. An elongated tail on the right side of the density curve is noticeable

in locations with medium and high space volume, which implies a higher probability of higher CO₂ levels. Figure 5e shows the density plot of CO₂ concentration for different volumes of indoor space aboard. The assigned subgroups follow extremely similar variations and trends for CO₂ concentration. This reaffirms that the venue dimensions do not have a significant impact on the incidence of high CO₂ concentration. Similar to the density plot from ceiling height sub-groups, an elongated tail on the right side of the density curve (towards higher CO₂ concentrations) is noticeable in locations with medium and high indoor space volume, and implies a higher probability of higher CO₂ level.

The experimental outcome illustrated that the influence of design conditions aboard, including room volume and ceiling height, on CO₂ concentrations remains unclear. Hence, a direct correlation between the variation of CO₂ concentration and ship indoor building design characteristics cannot be clearly established. However, results have indicated that increasing indoor space or room volume (floor surface area and ceiling height) does not directly correlate to an increase in VR, and suggested that other factors including the occupancy metric and ventilation performance may have a more significant impact on VR.

3.3.2 Sea and port days

Shore plug-in power refers to the vessel plugged into the local grid that utilises electricity supplied by the port (Port of Seattle, 2024) when docked at the seaport; instead of fully relying on marine fuels such as heavy fuel oil (HFO), marine diesel oil (MDO), or liquefied natural gas (LNG) (Merien-Paul et al., 2019). The utilisation of sufficient shore plug-in power while at berth will prevent the need for running auxiliary engines, and charge batteries for electric propulsion systems, meanwhile contributing to lower noise pollution, and greenhouse gas emissions (UK Chamber of Shipping, 2022), reducing CO₂ emission by up to 35% (Department for Transport, 2023). Langer et al. (2020) have found that the type of marine

fuel used can directly affect the IAQ on board a ship, as the ship intakes outdoor air for ventilation. In addition, apart from the direct impact of pollutants from emissions indoors (engine room and boiler room etc.), there is a high likelihood of outdoor air pollutants ingress from port areas, including exhaust gas emissions from marine traffic or land-based operations emissions, into the vessel's indoor environments (Guo et al., 2008; Leung, 2015; Guo et al., 2010). The vessel involved in the study is capable of using land-based power, however, at the time of monitoring the designated ports were not equipped with an onshore power system. This section therefore aims to discover whether traditional marine fuel and external environmental characteristics (sea and port) will affect indoor CO₂ concentrations.

Figure 6 shows the comparison of CO₂ concentrations for monitored locations on sea and port days. The 20-23 of August were specifically chosen since these were the days where a full available dataset with all locations being monitored. Data for the rest of the port days is presented in Figure S8. Figure 6a shows the comparison box plot between sea day (21 and 23.08.2023) and port day (20.08.2023) and Figure 6b shows the comparison box plot between sea day (21 and 23.08.2023) and port day (22.08.2023). The sea and port day data allows for the identification of potential differences in the indoor CO₂ concentrations between the berthing and sailing phases of a passenger cruise ship. Results presented in Figure 6 and Figure S8 only include data within the published arrival and sail times for each of the specific port days to ensure comparability (arrival and sail times for the port days have not been fully disclosed to remain anonymity for the ship.) There were noticeable grace periods between the published arrival and sail time, and the actual time of arrival and sailing. However, the timing period has not been recorded, therefore an estimation of one hour has been considered for pre-embarkation and post-disembarkation, assuming the cruise ship has either arrived at the port earlier or was leaving the port on time. For instance, the published arrival and sail times for

20.08.2023 were 07:00 and 14:00, hence, Figure 6a presents CO₂ concentrations data on board the cruise ship between 06:00-15:00.

Figure 6a shows that port day has a higher mean CO₂ concentration in general, except for the gym, bar and cabins. Figure 6b shows a similar result, indicating a higher mean CO₂ concentration on a port day for some parts of the cruise ship including the pub, buffet, and restaurant. Cabins have been excluded from the discussion for comparability purposes, because the cabin occupants (researcher) worked night shifts and took their rest in the morning during sea days. The buffet presented an elevated mean CO₂ concentration for all port days (Figure 6 and Figure S8), which could be attributed to the large outdoor area on deck 15, allowing outdoor pollutants' infiltration, as discussed in Section 3.1.1. The above results imply that depending on the docked port, some of the locations can be more prone to outdoor air pollutants ingress from the port areas, particularly dining areas (pub, restaurant and buffet). It is confirmed by the cruise company that the AC load normally does not change while berthed (except in extreme weather). Thus, assuming a common-sense hypothesis, passengers normally disembark the cruise ship for shore-side excursions when the vessel is berthed and there are fewer occupancies on board. It can be expected that passengers will typically spend the following amounts of time in different parts of the vessel: 1) cabins: passengers are expected to spend almost the same amount of time in cabins while in port or at sea, assuming most passengers do not spend much time in their cabins while at sea, apart from sleeping at night; 2) gym: passengers likely spend less time in the gym while in port as they are presumably on shore-side excursions; 3) theatre: passengers are typically back on board for the evening shows; 4) restaurant and buffet: passengers will typically take breakfast and dinner while in port; usually, only lunch is missed. However, in some ports, early dinner may also be taken ashore. 5) pub and bar: passengers will likely only occupy these spaces in the evening when they return from shore-side excursions, hence less occupancy is expected while in port. Thus, the above

results denote a high possibility that port-related exhaust emissions (including CO₂) from marine (and land) traffic or operations, given that modern vessels mainly operate on MDO, LNG and HFO (Clarke et al., 2023; European Commission, 2024; Sinay, 2023), could penetrate into the indoor ship environments. Cruise lines are suggested to pay extra attention to the ventilation configuration aboard during the hotelling period, because prolonged exposure to high concentrations of CO₂ can impose detrimental effects on human health (Azuma et al., 2018).

3.4 Ventilation performance

Table 4 shows the estimated mean ACH and ventilation rates, as well as descriptive statistics calculated at all monitored locations using the method outlined in Section 2.5. The actual occupancy data is not available due to limitations in logistics permissions, therefore the maximum occupancy for each location is used for the calculations. These ventilation rate estimates are to be provided as general guides to the overall performance of the space, because of a number of assumptions made around the homogenous distribution of the tracer gas (CO₂). Furthermore, it is assumed that there is no additional source of CO₂ during the period for the calculations of the decay; however, this could not be guaranteed in an operating cruise ship, especially for continuously operating venues.

The standard deviation refers to the distribution of the ACH and VR across the daily values calculated. The pub, buffet and bar close late at night, and therefore calculation of ventilation rates with decay from their closing hours is also not realistic, because CO₂ concentration is already low at that time. Random peaks are used for the calculations and are noted in Table S7. Similarly, for cabins, the decay trend is relatively unclear and random peaks are taken into account for calculations. The restaurant and theatre have relatively fixed operating hours, where guests will enter and leave at a specific time, such that clear peaks and decay of CO₂ can

be observed. Therefore, the decay CO_2 was calculated around their closing hours when occupants left the venue. Details of the calculation are summarised in Table S7.

The theatre shows elevated standard deviations for both ACH and VR. This could be attributed to a particular performance activity occurring (e.g. dancing and singing release more CO_2 concentrations than a comedy show) or possible usage of visual effects (smoke effect etc.). It might also indicate that the DCV was operating effectively. Cabins generally show lower standard deviations. However, a slightly elevated standard deviation appeared for cabin M due to the lower VR calculated for 23.08.2023. There could be two reasons for this, the first being that the cruise ship is on the way back to the UK port and the climate characteristics for the UK are typically colder than the Iberian Peninsula region. Therefore, occupants may have manually adjusted for less AC. Another reason could be that occupants (researchers) may have spent additional time in the room resting, at the end of the cruise and monitoring campaign.

The recommended guidelines introduced in Section 2.6 (Table 3) indicate ventilation flow rate standards ranging from $7.5\text{-}10 \text{ L s}^{-1} \text{ person}^{-1}$ for airborne disease mitigation. The buffet and restaurant did not comply with the suggested ventilation standards, with the buffet having the lowest VR, but still recording an acceptable IAQ (CO_2 level), suggesting that the actual occupancy in the buffet might have been less than what was used in the calculation (maximum occupancy). Similarly, the pub had excellent estimated VR but exhibited CO_2 concentrations below acceptable IAQ standards, exceeding 1500 ppm. This implies that the actual occupancy in the pub might have been more than what was used in the calculation, confirming our hypothesis that during peak sessions people could potentially be standing around the pub and the maximum occupancy exceeds the nominal/seated occupancy given by the cruise company. In addition, the data indicates that there might be locations that are over-ventilated, such as the theatre and the three cabins, with VR calculated up to $86 \text{ L s}^{-1} \text{ person}^{-1}$ (theatre) and $69 \text{ L s}^{-1} \text{ person}^{-1}$ (cabin M). However, the extremely high VR for cabins could be caused by the lower

occupancy level and the varying VR and ACH among each cabin are caused by the self-adjustable thermostat (AC). It is evident from the results above that occupancy has an impact on CO₂ distribution throughout the shipboard environment. However, the impact of the actual occupancy on CO₂ still requires further exploration to understand the resilience of ventilation provision in handling different occupancy levels.

3.4.1 Airborne infection probability

The infection probability for the two extreme emission scenarios where an infected individual is present in the sampling location speaking normally or loudly was estimated. It was assumed that the infected and susceptible individuals occupied the space together for the entire period and the initial concentration of virus present was assumed to be zero. The following assumptions were also made: (i) the virus emission rate for an infected individual speaking normally (SN) and speaking loudly (SL) are 9.4 quanta h⁻¹ and 60.5 quanta h⁻¹ respectively (Kumar et al., 2022; Mikszewski et al., 2020), (ii) facemasks were not worn at all times, and facemask efficiency has not been considered and (iii) the environment is fully mixed, and a Wells Riley model is applicable.

The potential relative risk of infection was calculated in the nine monitored locations aboard with air change rates obtained in Section 3.4, and the accumulated risk for different exposure times from 1-8 h. The infection transmission risk values for these scenarios are tabulated in Table S8. The infection risk estimate is based on a dynamic model that accounts for the build-up of the virus, hence, the indoor room volume and virus removal mechanisms heavily influence the risk of infection. The room volumes are summarised in Table 2. The results (Table S8) show that the overall risk of infection is low (8 h exposure for SN and SL: >3% and 7-17%, respectively), particularly in the theatre (8 h SL: <0.5%) this could be attributed to the higher VR across the vessel, which is reflected by the low CO₂ concentrations (Section 3.1).

Although the restaurant has been classified as band 4 for IAQ acceptance in Section 3.1, the probability of infection is surprisingly low, which means the high CO₂ recorded in the restaurant is mostly attributed to outliers (worst-case scenarios) and non-routine events causing sudden peaks.

The infection probabilities after 8 h exposure in the SL scenario at the gym and pub are 17.2% and 15.8%, respectively. However, it is important to note that it is less likely that passengers will be spending long periods in these locations. In fact, an approximately 2-3 h stay will be more realistic, which only accounts for a risk of infection of 5-7%. In terms of the cabins, due to the smaller room volume, certainly, the risk of infection when staying with an infected person is extremely high (up to 90%).

3.4.2 Energy effectiveness

The ventilation standards for airborne disease risk mitigation, introduced in Section 2.7, mainly emphasise a change for a continuous supply of 100% outdoor air, that can significantly affect HVAC energy consumption. Although higher ventilation rates typically act as a good strategy to reduce long-range transmission of airborne disease, the increased energy consumption associated with higher ventilation rates needs to be considered. Table 4 and Table S8 introduced the estimated mean ACH and ventilation rates, and the probability of airborne infection risk at the nine monitored locations aboard. Considering that the theatre (86 L s⁻¹ person⁻¹) and cabins (up to 69 L s⁻¹ person⁻¹) have largely exceeded the international standard recommended by professional institutions (7.5-10 L s⁻¹ person⁻¹; ASHRAE, 2023; CIBSE, 2021). These observations suggest that cruise ships should be considering a more comprehensive deployment or utilisation of a DCV. Both energy performance and IAQ can be improved by exploiting a DCV that adjusts the ventilation rate based on occupancy or CO₂ concentration in the microenvironment (Hesaraki and Holmberg, 2015; Laverge et al., 2011;

Zhang et al., 2021). This is particularly necessary for the theatre, with high VR and low probability of infectious risk (8 h exposure in SL and SN scenarios: 0.5% and >0.1%, respectively). Even though the sensors might be underestimating CO₂ concentrations in the theatre and consequently lead to higher estimated VR; due to the location of sensor and ventilation distribution setting, the primary aim of this study was to measure overall trends rather than localised variations. Furthermore, higher VR and ACH will genuinely be necessary for a larger indoor volume, it is believed there is an opportunity for primary energy saving by lowering hotel/AC load, while the ventilation performance will still post adequate IAQ and sufficient preparedness for infectious diseases.

4. Conclusions, limitations and future work

This study measured CO₂ concentrations, RH and temperature levels on board a cruise ship at sea. In addition, CO₂ levels in these environments have been used as a proxy to estimate the ventilation and airborne infectious transmission risk, as a result of co-exhalation of virus pathogen-laden particles by an infected person. The analysed data have then acted as an indicator for discussing the energy effectiveness of the ventilation provision on the cruise ship.

The key conclusions are outlined as follows:

- Coincidentally, most monitoring locations have found indoor CO₂ concentrations usually stay within set guidelines, which indicates that ventilation was sufficient relative to occupancy levels. The exception is for dining areas including the restaurant and pub (CO₂: >2000 ppm), suggesting that eating, drinking and social interaction between occupants, including possible loud discussion, could potentially increase occupants' emissions of CO₂.
- The sequential peaks in the CO₂ concentrations data imply that occupancy level had a significantly positive relation with the increase of CO₂ concentrations in shipboard

environments. The majority of the monitored locations (pub, buffet, restaurant and bar) have recorded peak CO₂ concentrations (peak hours) in the evening at around 21:00 and the evening period corresponds to the highest likely occupancy.

- Generally, a higher RH percentage of $68.2 \pm 5.3\%$ was found aboard compared to the typical ship design conditions ISO 7547. According to ASHRAE Standard 62.1 recommended targets, this also implies a considerable difference in the marine environment on board relative to land-based building environments. All monitored spaces have recorded a merely over air-conditioning phenomenon (range of temperature aboard recorded at $22.3 \pm 1.4^{\circ}\text{C}$), with some having an internal temperature as low as 20-21°C. Correlation between CO₂, temperature and RH, also denotes that thermal conditions are good indicators of higher occupancy.

- The actual influence of shipboard design conditions (volume and ceiling height) on CO₂ concentrations remains unclear. Results have indicated that larger indoor spaces or room volume do not directly correlate to an increase in VR, and suggested that other factors including the occupancy metric and ventilation performance may have a more significant impact on the VR.

- There is a noticeable increase in CO₂ concentration on board in some of the monitored sites during a port day. This phenomenon denotes that there is a high possibility that port-related exhaust emissions from the ship itself, as well as nearby marine and land traffic, are concentrated, leading to increased ambient CO₂ levels, and consequently ingress into the indoor ship environments.

- The assessment of ventilation performances showed overall excellent ventilation performance on board the cruise ship. Generally, dining areas (except the pub) have the poorest performances with less than $10 \text{ L s}^{-1} \text{ person}^{-1}$ of fresh air supply, and among them, the restaurant has the lowest ventilation and air change rates. In contrast, the

theatre and cabins can be considered as over-ventilated (average ventilation rates: theatre: 86 L s⁻¹ person⁻¹; cabin M: 69L s⁻¹ person⁻¹; cabin S: 35.5L s⁻¹ person⁻¹; cabin F: 22.6 L s⁻¹ person⁻¹).

- The estimated probability of airborne infection for an 8 h stay in a mass-gathering location for the SN scenario is low (<3%). Conversely, in the SL scenario, the probability of airborne infection is ranged from 7-17% (theatre: <0.1%). The gym and pub have accounted for the highest risk of infection in the SL scenarios at 17.2 % and 15.8 %, respectively.

The above conclusions allow to make the following recommendations:

- Reassess the current HVAC operation modes/configurations, as operational needs may be different in spaces supplied from the same AHU, to optimise ventilation provision from performance, IAQ, disease prevention and energy perspectives. Also, consider adjusting ACH corresponding to expected daily occupancy variations or peaks (e.g. pre-booking information in restaurants and shows) or thermal conditions (an alternative indicator of space occupancy).
- Consider increasing ventilation rates in parts of the cruise ship or ventilation upgrades for spaces that have lesser acceptance of IAQ levels, specifically dining areas. Also to contemplate the possibility of reducing over-air-conditioning/AC load in the cabins and gym (low internal temperatures of ~21°C), which could provide a relatively warmer climate to reduce the risk of virus survival and spread.
- Regular dehumidifying approaches can be considered in dining areas, to lower the RH to 40-60%, particularly in the restaurant and buffet with high RH percentages (>85%), where feasible as satisfactory thermal condition, and mould and disease control strategies. Emphasis focuses on implementing disease prevention protocols and

avoiding long hours of stay in the gym and pub when necessary, as the probability of airborne infection risk is relatively higher in these locations.

- Berthing phase: more attention to be paid regarding ventilation configuration to limit/dilute the ingress of outdoor exhaust emissions into the indoor ship environments (enhanced ventilation or filtering outdoor penetrated emissions), particularly for dining areas (pub, restaurant and buffet); Sailing phase: increase ventilation rates in the dining area . Providing an addition of fresh and clean air supply to typically high CO₂ concentrations dining areas to reduce the concentration of indoor air pollutants and the transmission of long-distance airborne contaminants in the face of infectious disease spreading events.
- Real-time pollution monitoring equipment should be deployed to enhance the completeness of the DCV system, for example, CO₂ and PM monitors. Indoor CO₂ sensors should be installed on a localised scale in different microenvironments aboard, to enable comprehensive data for the ventilation system to adjust accordingly when CO₂ exceeds the prescribed limits or to reduce ventilation for locations with smaller occupancy. In combination with PM, monitors can allow cruise companies to understand dust concentrations and the dispersion of airborne aerosol particles for decision-making on disease control and prevention strategies.

This work presents a unique dataset collected in different indoor ship-based environments in August 2023 during the post COVID-19 era, to build an understanding of the ventilation conditions and associated airborne disease transmission risk. In addition, this work demonstrates that data obtained from low-cost sensors is not limited to understanding IAQ and thermal conditions, but also infection risk and energy consumption evaluation. The study illustrates the importance of including measurements of thermal comfort factors and IAQ for ventilation performance studies. There is a need for continuous, long-term measurements of

passenger ships with different indoor design conditions/infrastructures, to build a comparative dataset at different sites and seasons of the year. These datasets would make a valuable contribution to understanding the infectious disease transmission risk related to ventilation conditions on board cruise ships. Such an evidence base would be invaluable for the development and validation of reliable computational fluid dynamics models of airborne respiratory aerosol dispersion within cruise ship environments, particularly in identifying locations that should be prioritised for further assessment and implementing disease prevention measures. It is also suggested to conduct more comprehensive work including attended monitoring, to reduce the time fraction that sensors record data during unoccupied hours, record the actual number of occupants, and obtain outdoor/ambient air quality data. In addition, the placement of sensors on cabinets close to the ceiling, while practical for minimising disruption and fluctuation/error of data, may have been influenced by obstructions and localised airflow patterns, potentially limiting their ability to detect spatial variations in IAQ. Future studies should consider deploying additional sensors in diverse locations to better capture spatial heterogeneity more comprehensively. Understanding these aspects is vital to first build a more robust recommendation for air quality and energy consumption optimisation on board large passenger ships, and more importantly, devise effective infection prevention and control strategies preparing the cruise ship industry for future pandemics like COVID-19.

Credit author statement

Ho Yin Wickson Cheung: Conceptualization, Data curation, Formal Analysis, Visualisation, Conceptualization, Writing - original draft, Writing - review and editing; **Prashant Kumar:** Conceptualization, Funding acquisition, Methodology, Project administration, Resources, Supervision, Visualization, Writing - Original Draft, Writing - review and editing; **Sarkawt Hama:** Data curation, Writing - original draft, Writing - review and editing; **Ana Paula Mendes Emygdioa:** Writing - review and editing; **Yingyue Wei:** Writing - review and editing;

Lemonia Anagnostopoulos: Writing - review and editing; **John Ewer:** Writing - review and editing; **Valerio Ferracci:** Writing - review and editing; **Edwin R Galea:** Writing - review and editing; **Angus Grandison:** Writing - review and editing; **Christos Hadjichristodoulou:** Funding, Writing - review and editing; **Fuchen Jia:** Writing - review and editing; **Pierfrancesco Lepore:** Writing - review and editing; **Lidia Morawska:** Writing - review and editing; **Varvara A Mouchtouri:** Writing - review and editing; **Niko Siilin:** Writing - review and editing; **Zhaozhi Wang:** Writing - review and editing. All the co-authors' names appear in alphabetical order after the core writing team. All authors have contributed to commenting on the draft manuscript and assisted in the cohesiveness and proofreading of this paper.

Acknowledgements

HEALTHY SAILING project has received funding from the European Union's Horizon Europe Framework Programme (HORIZON) under Grant Agreement number 101069764. Funded by the European Union. Views and opinions expressed are however those of the author(s) only and do not necessarily reflect those of the European Union or the European Climate, Infrastructure and Environment Executive Agency (CINEA) or the cruise company. Neither the European Union nor the granting authority can be held responsible for them. This work was funded by UK Research and Innovation (UKRI) under the UK government's Horizon Europe funding guarantee [grant numbers 10040786 and 10040720]. This work has received funding from the Swiss State Secretariat for Education, Research and Innovation (SERI).

Conflicts of Interest

The authors declare that there are no known competing financial interests or personal relationships that could have appeared to influence the work reported in this paper.

Appendix

935 the HEALTHY SAILING project collaborators: **Leonidas Kourentis**, European Scientific
 936 Association for Health and Hygiene in Maritime Transport (EU SHIPSAN Association),
 937 Greece; **Jörn Klein**, Department of Microsystems, Faculty of Technology, Natural Sciences
 938 and Maritime Sciences, University of Southeastern Norway, Norway; **Szava Julia Bansaghi**,
 939 Department of Microsystems, Faculty of Technology, Natural Sciences and Maritime Sciences,
 940 University of Southeastern Norway, Norway; **Volker Harth**, Institute for Occupational and
 941 Maritime Medicine, University Medical Center Hamburg-Eppendorf, Germany; **Jan Heidrich**,
 942 Institute for Occupational and Maritime Medicine, University Medical Center Hamburg-
 943 Eppendorf, Germany; **Johannes Neumann**, University Medical Center Hamburg-Eppendorf,
 944 Germany; **Symeon Nikolaou**, Department of Electrical Computer Engineering and
 945 Informatics, Frederick University, Cyprus; **Hannu Salmela**, VTT Technical Research Centre
 946 of Finland, Finland; **Nikolaos P. Ventikos**, School of Naval Architecture and Marine
 947 Engineering, National Technical University of Athens, Greece; **Carmen Varela**, National
 948 Centre of Epidemiology, Instituto de Salud Carlos III, Spain, CIBER in Epidemiology and
 949 Public Health (CIBERESP), Spain; **Maria Guerrero-Vadillo**, National Centre of
 950 Epidemiology, Instituto de Salud Carlos III, Spain, CIBER in Epidemiology and Public Health
 951 (CIBERESP), Spain; **Marina Peñuelas**, National Centre of Epidemiology, Instituto de Salud
 952 Carlos III, Spain, CIBER in Epidemiology and Public Health (CIBERESP), Spain; **Smaragda**
 953 **Reppa**, Department of Informatics and Telecommunications, National and Kapodistrian
 954 University of Athens, Greece; **Konstantinos Theofilis**, Department of Informatics and
 955 Telecommunications, National and Kapodistrian University of Athens, Greece; **Constantinos**
 956 **Tsibanis**, Department of Informatics and Telecommunications, National and Kapodistrian
 957 University of Athens, Greece; **Vassilis Papataxiarhis**, Department of Informatics and
 958 Telecommunications, National and Kapodistrian University of Athens, Greece; **Catalin Popa**,
 959 Romanian Naval Academy "Mircea cel Batran", Romania; **Sergiu Lupu**, Romanian Naval

Academy "Mircea cel Batran", Romania; **Filip Nistor**, Romanian Naval Academy "Mircea cel
 Batran", Romania; **Despoina Andrioti Bygyraa**, School of Public Health and Community
 Medicine, Department of Medicine, Sahlgrenska Academy, University of Gothenburg,
 Sweden; **Giorgio Guzzetta**, Fondazione Bruno Kessler, Italy; **Valentina Marziano**,
 Fondazione Bruno Kessler, Italy; **Goran Vukelić**, University of Rijeka, Faculty of Maritime
 Studies, Croatia; **Spyridon Athanasiadis**, Institute of Communication and Computer Systems
 (ICCS), Greece; **Stefanos Chatzimichelakis**, Institute of Communication and Computer
 Systems (ICCS), Greece; **Georgios Vosinakis**, Institute of Communication and Computer
 Systems (ICCS), Greece; **Dimitra Dionysiou**, Institute of Communication and Computer
 Systems (ICCS), Greece; **Eleftherios Ouzounoglou**, Institute of Communication and
 Computer Systems (ICCS), Greece; **Angelos Amditis**, Institute of Communication and
 Computer Systems (ICCS), Greece; **Vassilios Zagkas**, SimFWD, Greece; **Reuben D'Souza**,
 SimFWD, Greece; **Jürgen F Kolb**, Leibniz Institute for Plasma Science and Technology
 (INP), Germany; **Raphael Rataj**, Leibniz Institute for Plasma Science and Technology (INP),
 Germany; **Christine Zäadow**, Leibniz Institute for Plasma Science and Technology (INP),
 Germany; **Patrizio Pezzotti**, Istituto Superiore di Sanità, Italy; **Flavia Riccardo**, Istituto
 Superiore di Sanità, Italy.

References

- Aarnio, M., 2022. Cruise Ship Handbook (Vol. 14). Springer Nature. Available at:
<https://link.springer.com/book/10.1007/978-3-031-11629-2> (accessed: 16 September
 2024).
- Abe, H., Ushijima, Y., Amano, M., Sakurai, Y., Yoshikawa, R., Kinoshita, T., Kurosaki, Y.,
 Yanagihara, K., Izumikawa, K., Morita, K. and Kohno, S., 2022. Unique evolution of
 SARS-CoV-2 in the second large cruise ship cluster in Japan. *Microorganisms*, 10, 99.
- Abhijith, K.V., Kukadia, V. and Kumar, P., 2022. Investigation of air pollution mitigation
 measures, ventilation, and indoor air quality at three schools in London. *Atmospheric
 Environment*, 289, 119303.
- Adzic, F., Mustafa, M., Wild, O., Cheung, H.Y.W. and Epshtein, L.M., 2022, June. Post-
 Occupancy study of indoor air quality in university laboratories during the pandemic. In

989 Indoor Air 2022: 17th International Conference of the International Society of Indoor Air
990 Quality & Climate.

991 Adzic, F., Roberts, B.M., Hathway, E.A., Matharu, R.K., Ciric, L., Wild, O., Cook, M. and
992 Malki-Epshtein, L., 2022. A post-occupancy study of ventilation effectiveness from high-
993 resolution CO₂ monitoring at live theatre events to mitigate airborne transmission of SARS-
994 CoV-2. *Building and Environment*, 223, 109392.

995 Aganovic, A., Bi, Y., Cao, G., Drangsholt, F., Kurnitski, J. and Wargocki, P., 2021. Estimating
996 the impact of indoor relative humidity on SARS-CoV-2 airborne transmission risk using a
997 new modification of the Wells-Riley model. *Building and Environment*, 205, 108278.

998 Aller, J., Kuznetsova, M.R., Jahn, C. J., Kemp, P. 2005. The sea surface microlayer as a source
999 of viral and bacterial enrichment in marine aerosols. *Aerosol Science*, 36, 801–812.

1000 Almilaji, O., 2021. Air recirculation role in the spread of COVID-19 onboard the diamond
1001 princess cruise ship during a quarantine period. *Aerosol and Air Quality Research*, 21(4),
1002 200495-200495.

1003 Althouse, B.M., Wenger, E.A., Miller, J.C., Scarpino, S.V., Allard, A., Hébert-Dufresne, L.
1004 and Hu, H., 2020. Superspreading events in the transmission dynamics of SARS-CoV-2:
1005 Opportunities for interventions and control. *PLoS biology*, 18, 3000897.

1006 Angelova, R.A., Velichkova, R., Markov, D. and Stankov, P., 2022. The influence of the air
1007 temperature on the CO₂ emissions by occupants indoors. In *IOP Conference Series: Earth
1008 and Environmental Science* (Vol. 952, No. 1, p. 012012). IOP Publishing.

1009 American Society of Heating, Refrigerating and Air-Conditioning Engineers (ASHRAE)
1010 (2023). Standard 241, Control of Infectious Aerosols. Available at:
1011 [https://www.ashrae.org/about/news/2023/ashrae-publishes-standard-241-control-of-](https://www.ashrae.org/about/news/2023/ashrae-publishes-standard-241-control-of-infectious-aerosols)
1012 [infectious-aerosols](https://www.ashrae.org/about/news/2023/ashrae-publishes-standard-241-control-of-infectious-aerosols) (accessed: 21 August 2024).

1013 American Society of Heating, Refrigerating and Air-Conditioning Engineers (ASHRAE),
1014 2013. Standard 62.1-2013 Ventilation for acceptable indoor air quality. American Society
1015 of Heating, Refrigerating and Air-Conditioning Engineers, Inc., Atlanta, GA, p.40.

1016 Azuma, K., Kagi, N., Yanagi, U. and Osawa, H., 2018. Effects of low-level inhalation exposure
1017 to carbon dioxide in indoor environments: A short review on human health and
1018 psychomotor performance. *Environment International*, 121, 51-56.

1019 Bazant, M.Z., Kodio, O., Cohen, A.E., Khan, K., Gu, Z., Bush, J.W.M., 2021. Monitoring
1020 carbon dioxide to quantify the risk of indoor airborne transmission of COVID-19. *Flow* 1.

1021 Bhadoria, P., Gupta, G. and Agarwal, A., 2021. Viral pandemics in the past two decades: an
1022 overview. *Journal of family medicine and primary care*, 10(8), 2745-2750.

1023 Bozic, A., Kanduc, M. 2021. Relative humidity in droplet and airborne transmission of disease.
1024 *Journal of Biological Physics*, 47, 1–29.

1025 Brækken, A., Gabrielli, C. and Nord, N., 2023. Energy use and energy efficiency in cruise ship
1026 hotel systems in a Nordic climate. *Energy Conversion and Management*, 288, 117121.

1027 British Standards Institution (BSI), 2019. BS EN 16798-1:2019 - Energy performance of
1028 buildings. Ventilation for buildings - Indoor environmental input parameters for design and

1029 assessment of energy performance of buildings addressing indoor air quality, thermal
1030 environment, lighting and acoustics. Module M1-6. The British Standards Institution,
1031 London, UK.

1032 Buonanno, G., Stabile, L. and Morawska, L., 2020. Estimation of airborne viral emission:
1033 Quanta emission rate of SARS-CoV-2 for infection risk assessment. *Environment*
1034 *International*, 141, 105794.

1035 Buonanno, G., Morawska, L. and Stabile, L., 2020. Quantitative assessment of the risk of
1036 airborne transmission of SARS-CoV-2 infection: prospective and retrospective
1037 applications. *Environment International*, 145, 106112.

1038 Canha, N., Almeida, S.M., Freitas, M.C., Täubel, M. and Hänninen, O., 2013. Winter
1039 ventilation rates at primary schools: comparison between Portugal and Finland. *Journal of*
1040 *Toxicology and Environmental Health, Part A*, 76(6), 400-408.

1041 Chartered Institution of Building Services Engineers (CIBSE) (2021). COVID-19: Ventilation
1042 Version 5. Available at: <https://www.cibse.org/emerging-from-lockdown> (accessed: 26
1043 August 2024).

1044 Clarke, D., Chan, P., Dequeljoe, M., Kim, Y. and Barahona, S., 2023. CO₂ emissions from
1045 global shipping: A new experimental database. *OECD Statistics Working Papers*, No.
1046 2023/04, OECD Publishing, Paris, <https://doi.org/10.1787/bc2f7599-en>.

1047 Coulby, G., Clear, A.K., Jones, O. and Godfrey, A., 2021. Low-cost, multimodal
1048 environmental monitoring based on the Internet of Things. *Building and Environment*, 203,
1049 108014.

1050 Crews, C., Angwaawie, P., Abdul-Mumin, A., Yabasin, I.B., Attivor, E., Dibato, J. and Coffee,
1051 M.P., 2024. Assessing ventilation through ambient carbon dioxide concentrations across
1052 multiple healthcare levels in Ghana. *PLOS Global Public Health*, 4(8), e0003287.

1053 Cruise Lines International Association (CLIA) (2020). CLIA Announces Voluntary
1054 Suspension of Cruise Operations from U.S. Ports (USA). Available at:
1055 [https://cruising.org/en-gb/news-and-research/press-room/2020/june/clia-announces-](https://cruising.org/en-gb/news-and-research/press-room/2020/june/clia-announces-voluntary-suspension-of-cruise-operations-from-us-ports)
1056 [voluntary-suspension-of-cruise-operations-from-us-ports](https://cruising.org/en-gb/news-and-research/press-room/2020/june/clia-announces-voluntary-suspension-of-cruise-operations-from-us-ports) (accessed: 29 July 2024).

1057 Dai, H. and Zhao, B., 2020, December. Association of the infection probability of COVID-19
1058 with ventilation rates in confined spaces. In *Building Simulation* (Vol. 13, pp. 1321-1327).
1059 Tsinghua University Press.

1060 Deng, S. and Lau, J., 2019. Seasonal variations of indoor air quality and thermal conditions
1061 and their correlations in 220 classrooms in the Midwestern United States. *Building and*
1062 *Environment*, 157, 79-88.

1063 Department for Transport (2023) Call for evidence outcome, Use of maritime shore power in
1064 the UK: summary of call for evidence responses. Available at:
1065 [https://www.gov.uk/government/calls-for-evidence/use-of-maritime-shore-power-in-the-](https://www.gov.uk/government/calls-for-evidence/use-of-maritime-shore-power-in-the-uk-call-for-evidence/outcome/use-of-maritime-shore-power-in-the-uk-summary-of-call-for-evidence-responses)
1066 [uk-call-for-evidence/outcome/use-of-maritime-shore-power-in-the-uk-summary-of-call-](https://www.gov.uk/government/calls-for-evidence/use-of-maritime-shore-power-in-the-uk-call-for-evidence/outcome/use-of-maritime-shore-power-in-the-uk-summary-of-call-for-evidence-responses)
1067 [for-evidence-responses](https://www.gov.uk/government/calls-for-evidence/use-of-maritime-shore-power-in-the-uk-call-for-evidence/outcome/use-of-maritime-shore-power-in-the-uk-summary-of-call-for-evidence-responses) (accessed: 20 June 2024).

1068 Edwards, N.J., Widrick, R., Wilmes, J., Breisch, B., Gerschefske, M., Sullivan, J., Potember,
1069 R. and Espinoza-Calvio, A., 2021. Reducing COVID-19 airborne transmission risks on

1070 public transportation buses: An empirical study on aerosol dispersion and control. *Aerosol*
1071 *Science and Technology*, 55(12), 1378-1397.

1072 EMG and SPI-B, 2021. Application of CO₂ monitoring as an approach to managing ventilation
1073 to mitigate SARS-COV-2 transmission, 27 May 2021 - GOV.UK. Available at:
1074 [https://www.gov.uk/government/publications/emg-and-spi-b-application-of-co2-](https://www.gov.uk/government/publications/emg-and-spi-b-application-of-co2-monitoring-as-an-approach-to-managing-ventilation-to-mitigate-sars-cov-2-transmission-27-may-2021)
1075 [monitoring-as-an-approach-to-managing-ventilation-to-mitigate-sars-cov-2-transmission-](https://www.gov.uk/government/publications/emg-and-spi-b-application-of-co2-monitoring-as-an-approach-to-managing-ventilation-to-mitigate-sars-cov-2-transmission-27-may-2021)
1076 [27-may-2021](https://www.gov.uk/government/publications/emg-and-spi-b-application-of-co2-monitoring-as-an-approach-to-managing-ventilation-to-mitigate-sars-cov-2-transmission-27-may-2021) (accessed: 30 October 2023).

1077 European Commission (2024). Reducing emissions from the shipping sector. Available at:
1078 [https://climate.ec.europa.eu/eu-action/transport/reducing-emissions-shipping-](https://climate.ec.europa.eu/eu-action/transport/reducing-emissions-shipping-sector_en#:~:text=While%20maritime%20transport%20plays%20an%20essential%20role,were%20responsible%20for%20around%202.9%%20of%20global)
1079 [sector_en#:~:text=While%20maritime%20transport%20plays%20an%20essential%20rol](https://climate.ec.europa.eu/eu-action/transport/reducing-emissions-shipping-sector_en#:~:text=While%20maritime%20transport%20plays%20an%20essential%20role,were%20responsible%20for%20around%202.9%%20of%20global)
1080 [e,were%20responsible%20for%20around%202.9%%20of%20global](https://climate.ec.europa.eu/eu-action/transport/reducing-emissions-shipping-sector_en#:~:text=While%20maritime%20transport%20plays%20an%20essential%20role,were%20responsible%20for%20around%202.9%%20of%20global) (accessed: 22 August
1081 2024).

1082 Fang, L., Clausen, G. and Fanger, P.O., 1998. Impact of temperature and humidity on the
1083 perception of indoor air quality. *Indoor Air*, 8(2), 80-90.

1084 Fantozzi, F., Lamberti, G., Leccese, F. and Salvadori, G., 2022. Monitoring CO₂ concentration
1085 to control the infection probability due to airborne transmission in naturally ventilated
1086 university classrooms. *Architectural Science Review*, 65(4), 306-318.

1087 Federation of European Heating, Ventilation and Air Conditioning Associations (REHVA)
1088 (2021). COVID-19 Guidance. Available at: [https://www.rehva.eu/activities/covid-19-](https://www.rehva.eu/activities/covid-19-guidance/rehva-covid-19-guidance)
1089 [guidance/rehva-covid-19-guidance](https://www.rehva.eu/activities/covid-19-guidance/rehva-covid-19-guidance) (accessed: 19 May 2024).

1090 Frieden, T.R. and Lee, C.T., 2020. Identifying and interrupting superspreading events—
1091 implications for control of severe acute respiratory syndrome coronavirus 2. *Emerging*
1092 *Infectious Diseases*, 26, 1059.

1093 Global Monitoring Laboratory (GML) (2024) Trends in Atmospheric Carbon Dioxide (CO₂).
1094 Available at: <https://gml.noaa.gov/ccgg/trends/> (accessed: 21 August 2024).

1095 Guagliardo, S.A.J., Prasad, P.V., Rodriguez, A., Fukunaga, R., Novak, R.T., Ahart, L.,
1096 Reynolds, J., Griffin, I., Wiegand, R., Quilter, L.A. and Morrison, S., 2022. Cruise ship
1097 travel in the era of coronavirus disease 2019 (COVID-19): a summary of outbreaks and a
1098 model of public health interventions. *Clinical Infectious Diseases*, 74(3), 490-497.

1099 Guo, H., Morawska, L., He, C. and Gilbert, D., 2008. Impact of ventilation scenario on air
1100 exchange rates and on indoor particle number concentrations in an air-conditioned
1101 classroom. *Atmospheric Environment*, 42(4), 757-768.

1102 Guo, H., Morawska, L., He, C., Zhang, Y.L., Ayoko, G. and Cao, M., 2010. Characterization
1103 of particle number concentrations and PM 2.5 in a school: Influence of outdoor air pollution
1104 on indoor air. *Environmental Science and Pollution Research*, 17, 1268-1278.

1105 Guo, L., Yang, Z., Zhang, L., Wang, S., Bai, T., Xiang, Y. and Long, E., 2021. Systematic
1106 review of the effects of environmental factors on virus inactivation: implications for
1107 coronavirus disease 2019. *International Journal of Environmental Science and Technology*,
1108 18, 2865-2878.

- 1109 Hama, S., Kumar, P., Tiwari, A., Wang, Y. and Linden, P.F., 2023. The underpinning factors
1110 affecting the classroom air quality, thermal comfort and ventilation in 30 classrooms of
1111 primary schools in London. *Environmental Research*, 236, 116863.
- 1112 Health and Safety Executive (HSE) (2023). Temperature: Thermal comfort. Available at:
1113 <https://www.hse.gov.uk/temperature/thermal/#:~:text=You%20should%20provide%20a%20minimum,it's%20too%20hot%20to%20work>. (accessed: 20 February 2024).
1114
- 1115 Hesarakı, A. and Holmberg, S., 2015. Demand-controlled ventilation in new residential
1116 buildings: Consequences on indoor air quality and energy savings. *Indoor and Built
1117 Environment*, 24(2), 162-173.
- 1118 HOBO, 2015. HOBO® MX CO₂ Logger (MX1102) Manual. Onset Computer Corporation,
1119 19198-J. (accessed on 30/10/2023.)
- 1120 ISO, 2022. ISO 7547:2022. Ships and marine technology. Air-conditioning and ventilation of
1121 accommodation spaces and other enclosed compartments on board ships. Design
1122 conditions and basis of calculations.
- 1123 Jayaweera, M., Perera, H., Gunawardana, B. and Manatunge, J., 2020. Transmission of
1124 COVID-19 virus by droplets and aerosols: A critical review on the unresolved dichotomy.
1125 *Environmental Research*, 188, 109819.
- 1126 Jones, E.R., Cedeño Laurent, J.G., Young, A.S., Coull, B.A., Spengler, J.D. and Allen, J.G.,
1127 2022. Indoor humidity levels and associations with reported symptoms in office buildings.
1128 *Indoor Air*, 32(1), e12961.
- 1129 Kaushik, A., Arif, M., Tumula, P. and Ebohon, O.J., 2020. Effect of thermal comfort on
1130 occupant productivity in office buildings: Response surface analysis. *Building and
1131 Environment*, 180, 107021.
- 1132 Kim, S.S. and Lee, Y.G., 2010. Field measurements of indoor air pollutant concentrations on
1133 two new ships. *Building and Environment*, 45, 2141-2147.
- 1134 Kosako, M. and Shiiyama, K., 2008. Introduction of air-conditioning system design for a large
1135 cruise ship: Princess Cruises Mitsubishi Grand Series implementation example. *Journal of
1136 the Japan Society of Naval and Ocean Engineers*, 17, 24-26.
- 1137 Kumar, P., Hama, S., Abbass, R.A., Abhijith, K.V., Tiwari, A., Grassie, D., & Mitsakou, C.,
1138 2024. Environmental quality in sixty primary school classrooms in London. *Journal of
1139 Building Engineering* 91, 109549.
- 1140 Kumar, P., Hama, S., Abbass, R. A., Nogueira, T., Brand, V. S., Wu, H.W., Abulude, F. O.,
1141 Adelodun, A. A., de Fatima Andrade, M., Asfaw, A., Aziz, K. H., Cao, S. J., El-Gendy, A.,
1142 Indu, G., Kehbila, A. G., Mustafa, F., Muula, A. S., Nahian, S., Nardocci, A. C., Nelson,
1143 W., Ngowi, A. V., Olaya, Y., Omer, K., Osanoh, P., Salam, A., Nagendra SM, S., 2022.
1144 CO₂ exposure, ventilation, thermal comfort, and health risks in low-income home kitchens
1145 of twelve global cities. *Journal of Building Engineering* 61,105254.
- 1146 Kumar, P., Hama, S., Cheung, H.Y.W., Anagnostopoulos, L., Hadjichristodoulou, C.,
1147 Mouchtouri, V.A., Kourentis, L., Wang, Z., Galea, E.R., Ewer, J., Grandison, A., Jia, F.
1148 and Siilin, N., 2024. Airborne Pathogen Monitoring and Dispersion Modelling on
1149 Passenger Ships: A Review. In preparation.

- 1150 Kumar, P., Kalaivasan, G., Bhagat, R.K., Mumby, S., Adcock, I.M., Porter, A.E., Ransome,
1151 E., Abubakar-Waziri, H., Bhavsar, P., Shishodia, S., Dilliway, C., Fang, F., Pain, C.C.,
1152 Chung, K.F., 2022. Active Air Monitoring for Understanding the Ventilation and Infection
1153 Risks of SARS-CoV-2 Transmission in Public Indoor Spaces. *Atmosphere (Basel)* 13.
- 1154 Kumar, P., Rawat, N. and Tiwari, A., 2023. Micro-characteristics of a naturally ventilated
1155 classroom air quality under varying air purifier placements. *Environmental Research*, 217,
1156 114849
- 1157 Langer, S., Österman, C., Strandberg, B., Moldanová, J. and Fridén, H., 2020. Impacts of fuel
1158 quality on indoor environment onboard a ship: From policy to practice. *Transportation
1159 Research Part D: Transport and Environment*, 83, 102352.
- 1160 Laverge, J., Van Den Bossche, N., Heijmans, N. and Janssens, A., 2011. Energy saving
1161 potential and repercussions on indoor air quality of demand controlled residential
1162 ventilation strategies. *Building and Environment*, 46(7), 1497-1503.
- 1163 Leung, D.Y., 2015. Outdoor-indoor air pollution in urban environment: challenges and
1164 opportunity. *Frontiers in Environmental Science*, 2, 69.
- 1165 Li, C. and Tang, H., 2022. Comparison of COVID-19 infection risks through aerosol
1166 transmission in supermarkets and small shops. *Sustainable Cities and Society*, 76, 103424.
- 1167 Malki-Epshtein, L., Cook, M., Hathway, A., Adzic, F., Iddon, C., Roberts, B.M. and Mustafa,
1168 M., 2022. Application of CO₂ monitoring methods for post-occupancy evaluation of
1169 ventilation effectiveness to mitigate airborne disease transmission at events. In *Chartered
1170 Institution of Building Services Engineers (CIBSE): CIBSE Technical Symposium 2022*.
- 1171 Malki-Epshtein, L., Stoesser, T., Ciric, L., Stubbs, A., Tyler, N., 2020. Report on Scientific
1172 advice to TfL on bus driver assault screen modifications due to the Covid-19 pandemic,
1173 UCL Department of Civil, Environmental and Geomatic Engineering, London, UK.
1174 Available at: [https://www.ucl.ac.uk/civil-environmental-geomatic-engineering/sites/civil-
1175 environmental-geomatic-
1176 engineering/files/tfl_drivers_cab_modifications_ucl_full_report_2020-10-28_0.pdf](https://www.ucl.ac.uk/civil-environmental-geomatic-engineering/sites/civil-environmental-geomatic-engineering/files/tfl_drivers_cab_modifications_ucl_full_report_2020-10-28_0.pdf).
1177 (accessed: 29 May 2024).
- 1178 Mao, N., Zhang, D., Li, Y., Li, Y., Li, J., Zhao, L., Wang, Q., Cheng, Z., Zhang, Y. and Long,
1179 E., 2023. How do temperature, humidity, and air saturation state affect the COVID-19
1180 transmission risk?. *Environmental Science and Pollution Research*, 30(2), 3644-3658.
- 1181 Mecnas, P., Bastos, R.T.D.R.M., Vallinoto, A.C.R. and Normando, D., 2020. Effects of
1182 temperature and humidity on the spread of COVID-19: A systematic review. *PLoS one*,
1183 15(9), e0238339.
- 1184 Merien-Paul, R.H., Enshaei, H. and Jayasinghe, S.G., 2019. Effects of fuel-specific energy and
1185 operational demands on cost/emission estimates: A case study on heavy fuel-oil vs
1186 liquefied natural gas. *Transportation Research Part D: Transport and Environment*, 69, 77-
1187 89.
- 1188 Mihai, V. and Rusu, L., 2021. An overview of the ship ventilation systems and measures to
1189 avoid the spread of diseases. *Inventions*, 6(3), 55.

1190 Mikszewski, A., Buonanno, G., Stabile, L., Pacitto, A. and Morawska, L., 2020. Airborne
 1191 infection risk calculator. Available at:
 1192 [https://www.makingmusic.org.uk/sites/makingmusic.org.uk/files/AIRC-Users-Manual-](https://www.makingmusic.org.uk/sites/makingmusic.org.uk/files/AIRC-Users-Manual-1.0-July-2020.pdf)
 1193 [1.0-July-2020.pdf](https://www.makingmusic.org.uk/sites/makingmusic.org.uk/files/AIRC-Users-Manual-1.0-July-2020.pdf) (accessed: 16 September 2024).

1194 Miller, S.L., Nazaroff, W.W., Jimenez, J.L., Boerstra, A., Buonanno, G., Dancer, S.J.,
 1195 Kurnitski, J., Marr, L.C., Morawska, L. and Noakes, C., 2021. Transmission of SARS-
 1196 CoV-2 by inhalation of respiratory aerosol in the Skagit Valley Chorale superspreading
 1197 event. *Indoor Air*, 31(2), 314-323.

1198 Morawska, L. and Cao, J., 2020. Airborne transmission of SARS-CoV-2: The world should
 1199 face the reality. *Environment International*, 139, 105730.

1200 Muelas, Á., Remacha, P., Pina, A., Tizné, E., El-Kadmiri, S., Ruiz, A., Aranda, D. and
 1201 Ballester, J., 2022. Analysis of different ventilation strategies and CO₂ distribution in a
 1202 naturally ventilated classroom. *Atmospheric Environment*, 283, 119176.

1203 Noti, J.D., Blachere, F.M., McMillen, C.M., Lindsley, W.G., Kashon, M.L., Slaughter, D.R.
 1204 and Beezhold, D.H., 2013. High humidity leads to loss of infectious influenza virus from
 1205 simulated coughs. *PloS one*, 8(2), e57485.

1206 Nottmeyer, L., Armstrong, B., Lowe, R., Abbott, S., Meakin, S., O'Reilly, K.M., von Borries,
 1207 R., Schneider, R., Royé, D., Hashizume, M. and Pascal, M., 2023. The association of
 1208 COVID-19 incidence with temperature, humidity, and UV radiation—A global multi-city
 1209 analysis. *Science of The Total Environment*, 854, 158636.

1210 Park, S. and Song, D., 2023. CO₂ concentration as an indicator of indoor ventilation
 1211 performance to control airborne transmission of SARS-CoV-2. *Journal of Infection and*
 1212 *Public Health*, 16(7), 1037-1044.

1213 Peng, Z. and Jimenez, J.L., 2021. Exhaled CO₂ as a COVID-19 infection risk proxy for
 1214 different indoor environments and activities. *Environmental Science & Technology*
 1215 *Letters*, 8, 392-397.

1216 Perry, R.J., Lyu, K., Dong, J., Li, X., Yang, Y., Qing, H., Wang, A., Yang, X. and Shulman,
 1217 G.I., 2020. Leptin mediates postprandial increases in body temperature through
 1218 hypothalamus–adrenal medulla–adipose tissue crosstalk. *The Journal of Clinical*
 1219 *Investigation*, 130.

1220 Port of Seattle (2024). Cruise Ship Shore Power Facts. Available at:
 1221 <https://www.portseattle.org/page/cruise-ship-shore-power-facts#> (accessed: 13 June 2024).

1222 Q-TRAK, 2016. Q-TRAK™ Indoor air quality monitor model 7575. Operation and service
 1223 manual, TSI Incorporated, p/n 6004850, revision F, 2016.

1224 Ren, C., Zhu, H.C. and Cao, S.J., 2022. Ventilation strategies for mitigation of infection disease
 1225 transmission in an indoor environment: a case study in office. *Buildings*, 12(2), 180.

1226 Satish, U., Mendell, M.J., Shekhar, K., Hotchi, T., Sullivan, D., Streufert, S. and Fisk, W.J.,
 1227 2012. Is CO₂ an indoor pollutant? Direct effects of low-to-moderate CO₂ concentrations on
 1228 human decision-making performance. *Environmental Health Perspectives*, 120(12), 1671-
 1229 1677.

1230 Schade, W., Reimer, V., Seipenbusch, M. and Willer, U., 2021. Experimental investigation of
1231 aerosol and CO₂ dispersion for evaluation of COVID-19 infection risk in a concert
1232 hall. *International Journal of Environmental Research and Public Health*, 18(6), 3037.

1233 Schibuola, L. and Tambani, C., 2020. Indoor environmental quality classification of school
1234 environments by monitoring PM and CO₂ concentration levels. *Atmospheric Pollution*
1235 *Research*, 11(2), 332-342.

1236 Schmeling, D., Kühn, M., Schiepel, D., Dannhauer, A., Lange, P., Kohl, A., Niehaus, K.,
1237 Berlitz, T., Jäckle, M., Kwitschinski, T. and Tielkes, T., 2022. Analysis of aerosol
1238 spreading in a German Inter City Express (ICE) train carriage. *Building and*
1239 *Environment*, 222, 109363.

1240 Setti, L., Passarini, F., De Gennaro, G., Barbieri, P., Perrone, M.G., Borelli, M., Palmisani, J.,
1241 Di Gilio, A., Piscitelli, P. and Miani, A., 2020. Airborne transmission route of COVID-19:
1242 why 2 meters/6 feet of inter-personal distance could not be enough. *International Journal*
1243 *of Environmental Research and Public Health*, 17(8), 2932.

1244 Sinay (2023). How much does the shipping industry contribute to global CO₂ emissions?.
1245 Available at: [https://sinay.ai/en/how-much-does-the-shipping-industry-contribute-to-](https://sinay.ai/en/how-much-does-the-shipping-industry-contribute-to-global-co2-emissions/#:~:text=Utilizing%20slow%20steaming%20to%20reduce,consumption%20and%20greenhouse%20gas%20emissions)
1246 [global-co2-](https://sinay.ai/en/how-much-does-the-shipping-industry-contribute-to-global-co2-emissions/#:~:text=Utilizing%20slow%20steaming%20to%20reduce,consumption%20and%20greenhouse%20gas%20emissions)
1247 [emissions/#:~:text=Utilizing%20slow%20steaming%20to%20reduce,consumption%20an](https://sinay.ai/en/how-much-does-the-shipping-industry-contribute-to-global-co2-emissions/#:~:text=Utilizing%20slow%20steaming%20to%20reduce,consumption%20and%20greenhouse%20gas%20emissions)
1248 [d%20greenhouse%20gas%20emissions](https://sinay.ai/en/how-much-does-the-shipping-industry-contribute-to-global-co2-emissions/#:~:text=Utilizing%20slow%20steaming%20to%20reduce,consumption%20and%20greenhouse%20gas%20emissions) (accessed: 22 August 2024).

1249 Sun J., Jin, Z., Chang, H., Zhang, W. 2024. A review of chloride transport in concrete exposed
1250 to the marine atmosphere zone environment: Experiments and numerical models. *Journal*
1251 *of Building Engineering*, 84, 108591.

1252 Sze To, G.N. and Chao, C.Y.H., 2010. Review and comparison between the Wells–Riley and
1253 dose-response approaches to risk assessment of infectious respiratory diseases. *Indoor Air*,
1254 20(1), 2-16.

1255 Tang, S., Mao, Y., Jones, R.M., Tan, Q., Ji, J.S., Li, N., Shen, J., Lv, Y., Pan, L., Ding, P. and
1256 Wang, X., 2020. Aerosol transmission of SARS-CoV-2? Evidence, prevention and control.
1257 *Environment International*, 144, 106039.

1258 UK Chamber of Shipping (2022) UK Chamber of Shipping's Position on Shore Power.
1259 Available at:
1260 [https://www.ukchamberofshipping.com/sites/default/files/Shore_Power_Position_Paper_-_](https://www.ukchamberofshipping.com/sites/default/files/Shore_Power_Position_Paper_-_endorsed_by_SB_22.4.22.pdf)
1261 [endorsed_by_SB_22.4.22.pdf](https://www.ukchamberofshipping.com/sites/default/files/Shore_Power_Position_Paper_-_endorsed_by_SB_22.4.22.pdf) (accessed: 20 June 2024).

1262 UNWTO (2021). COVID-19 and Tourism: 2020: A year in review. Available at:
1263 <https://www.unwto.org/covid-19-and-tourism-2020> (accessed: 29 July 2024).

1264 Verheyen, C.A. and Bourouiba, L., 2022. Associations between indoor relative humidity and
1265 global COVID-19 outcomes. *Journal of the Royal Society Interface*, 19(196), 20210865.

1266 Villanueva, F., Notario, A., Cabañas, B., Martín, P., Salgado, S. and Gabriel, M.F., 2021.
1267 Assessment of CO₂ and aerosol (PM_{2.5}, PM₁₀, UFP) concentrations during the reopening
1268 of schools in the COVID-19 pandemic: The case of a metropolitan area in Central-Southern
1269 Spain. *Environmental Research*, 197, 111092.

1270 Wang, C.C., Prather, K.A., Sznitman, J., Jimenez, J.L., Lakdawala, S.S., Tufekci, Z. and Marr,
1271 L.C., 2021. Airborne transmission of respiratory viruses. *Science*, 373(6558), eabd9149.

1272 Wang, Z., Cao, M., Tang, H., Dong, B., Ji, Y. and Han, F., 2024. Marine temperature and
1273 humidity regulation combined system: performance analysis and multi-objective
1274 optimization. *Case Studies in Thermal Engineering*, 56, 104215.

1275 Wang, Z., Galea, E.R., Grandison, A., Ewer, J. and Jia, F., 2021. Inflight transmission of
1276 COVID-19 based on experimental aerosol dispersion data. *Journal of Travel Medicine*,
1277 28(4), taab023.

1278 Wang, Z., Galea, E.R., Grandison, A., Ewer, J. and Jia, F., 2022. A coupled Computational
1279 Fluid Dynamics and Wells-Riley model to predict COVID-19 infection probability for
1280 passengers on long-distance trains. *Safety Science*, 147, 105572.

1281 WHO (2023). Statement on the fifteenth meeting of the IHR (2005) Emergency Committee on
1282 the COVID-19 pandemic. Available at: [https://www.who.int/news/item/05-05-2023-](https://www.who.int/news/item/05-05-2023-statement-on-the-fifteenth-meeting-of-the-international-health-regulations-(2005)-emergency-committee-regarding-the-coronavirus-disease-(covid-19)-pandemic)
1283 [statement-on-the-fifteenth-meeting-of-the-international-health-regulations-\(2005\)-](https://www.who.int/news/item/05-05-2023-statement-on-the-fifteenth-meeting-of-the-international-health-regulations-(2005)-emergency-committee-regarding-the-coronavirus-disease-(covid-19)-pandemic)
1284 [emergency-committee-regarding-the-coronavirus-disease-\(covid-19\)-pandemic](https://www.who.int/news/item/05-05-2023-statement-on-the-fifteenth-meeting-of-the-international-health-regulations-(2005)-emergency-committee-regarding-the-coronavirus-disease-(covid-19)-pandemic) (accessed:
1285 29 May 2024).

1286 Woodward, H., De Kreijl, R.J., Kruger, E.S., Fan, S., Tiwari, A., Hama, S., Noel, S., Davies
1287 Wykes, M.S., Kumar, P. and Linden, P.F., 2022. An evaluation of the risk of airborne
1288 transmission of COVID-19 on an inter-city train carriage. *Indoor Air*, 32(10), e13121.

1289 Woodward, H., Fan, S., Bhagat, R.K., Dadonau, M., Wykes, M.D., Martin, E., Hama, S.,
1290 Tiwari, A., Dalziel, S.B., Jones, R.L. and Kumar, P., 2021. Air flow experiments on a train
1291 carriage—towards understanding the risk of airborne transmission. *Atmosphere*, 12(10),
1292 1267.

1293 Xu, P., Qian, H., Miao, T., Yen, H.L., Tan, H., Kang, M., Cowling, B.J. and Li, Y., 2020.
1294 Transmission routes of Covid-19 virus in the Diamond Princess Cruise ship. *MedRxiv*,
1295 2020-04.

1296 Yan, Y., Li, X., Shang, Y. and Tu, J., 2017. Evaluation of airborne disease infection risks in an
1297 airliner cabin using the Lagrangian-based Wells-Riley approach. *Building and*
1298 *Environment*, 121, 79-92.

1299 Yin, H., Zhai, X., Ning, Y., Li, Z., Ma, Z., Wang, X. and Li, A., 2022. Online monitoring of
1300 PM_{2.5} and CO₂ in residential buildings under different ventilation modes in Xi'an city.
1301 *Building and Environment*, 207, 108453.

1302 Zhang, J., Qin, F., Qin, X., Li, J., Tian, S., Lou, J., Kang, X., Lian, H., Niu, S., Zhang, W. and
1303 Chen, Y., 2021. Transmission of SARS-CoV-2 during air travel: a descriptive and
1304 modelling study. *Annals of Medicine*, 53(1), 1569-1575.

1305 Zhang, S., Ai, Z. and Lin, Z., 2021. Novel demand-controlled optimization of constant-air-
1306 volume mechanical ventilation for indoor air quality, durability and energy saving. *Applied*
1307 *Energy*, 293, 116954.

1308 Zhu, P., Tan, X., Wang, M., Guo, F., Shi, S., Li, Z., 2023. The impact of mass gatherings on
1309 the local transmission of COVID-19 and the implications for social distancing policies:
1310 Evidence from Hong Kong. *PLoS One* 18.

List of Figures

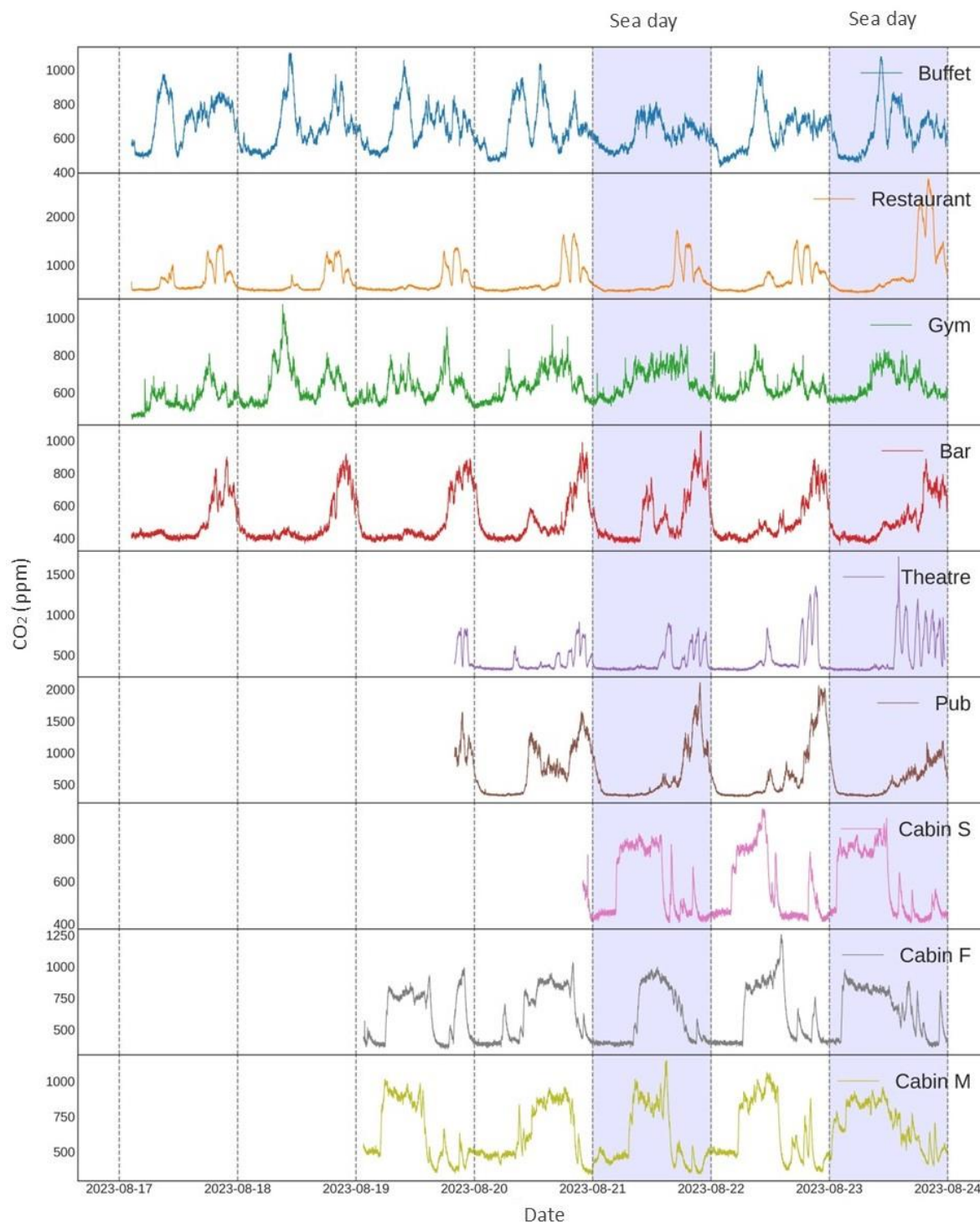
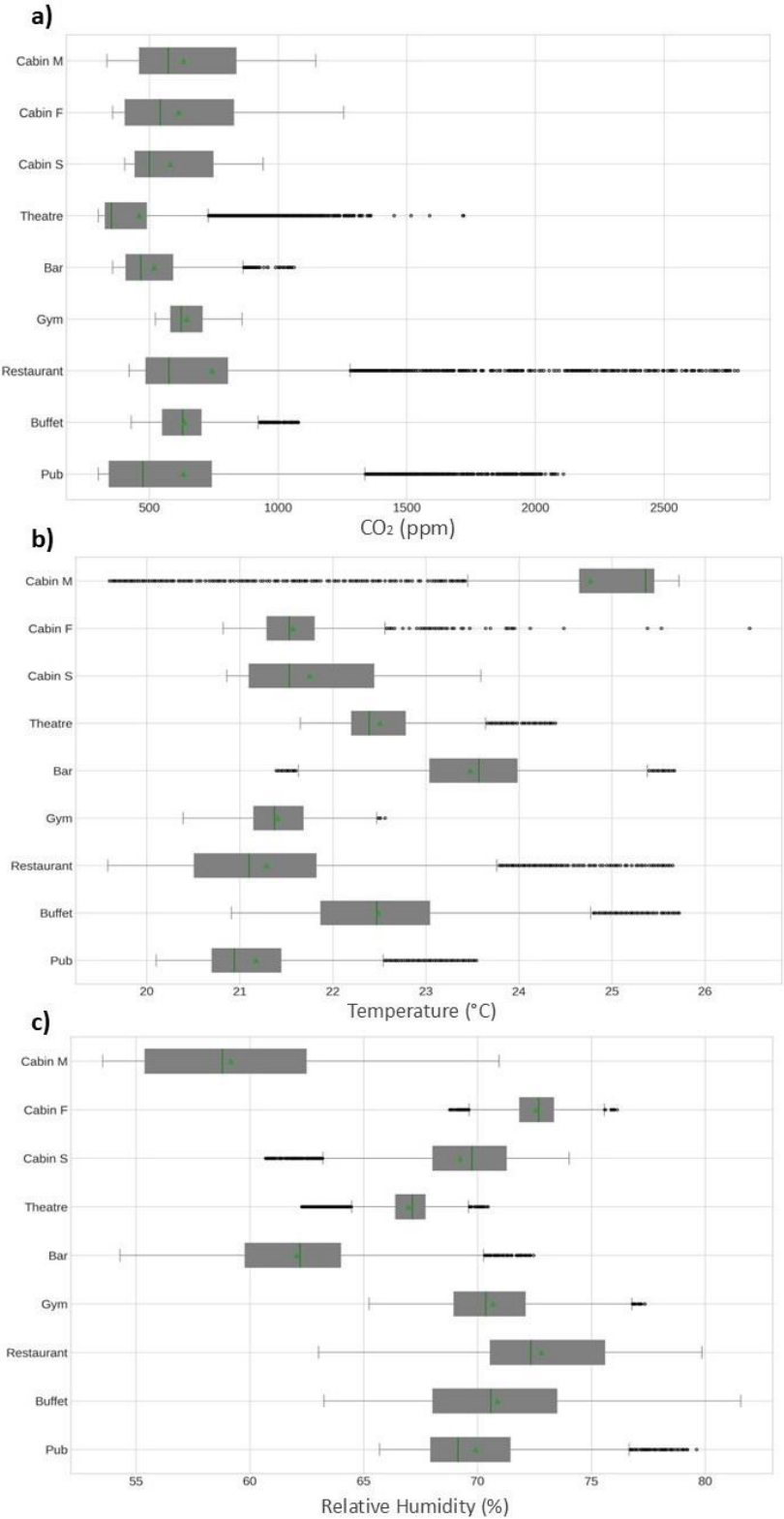


Figure 1. Full-time series of CO₂ concentrations (ppm) at all monitored locations during different study phases. Data is presented from 16-24.08.2023 and is recorded at a 1-minute resolution. The blue highlighted sections represent the days when the vessel was sailing (sea day: 21.08.2023 and 23.08.2023).

1318
1319



1320
1321 **Figure 2.** (a) Box plot for CO₂ concentrations (ppm); (b) Box plot for temperature (°C); (c)
1322 Box plot for relative humidity (%), at all monitored locations. The box plots denote the
1323 interquartile range, the lower quartile (Q₁), the median in the middle green line (Q₂), and the

third quartile (Q_3). The plot also includes the mean (shown by the green rectangle), minimum (Q_0) maximum (Q_4) (bottom and the top edge of the whiskers) and the outliers (black dots).

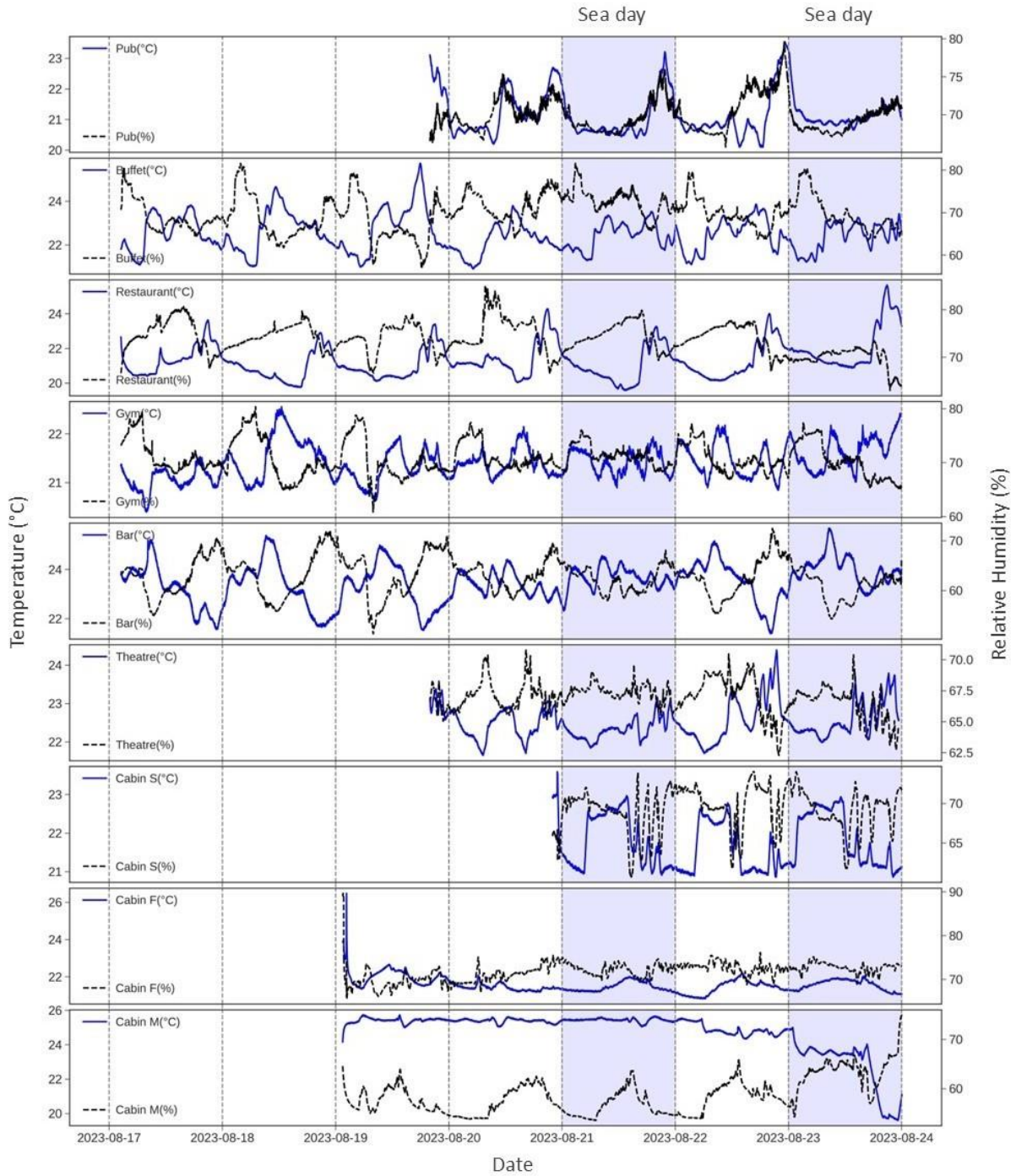


Figure 3. Full-time series of temperature and relative humidity at all monitored locations during different study phases. Data is presented from 16-24.08.2023 and is recorded at one-minute intervals. The blue line and black line represent temperature (left y-axis, °C) and RH (right y-axis, %) respectively. The blue highlighted sections represent the days that the cruise ship was sailing (sea days: 21.08.2023 and 23.08.2023).

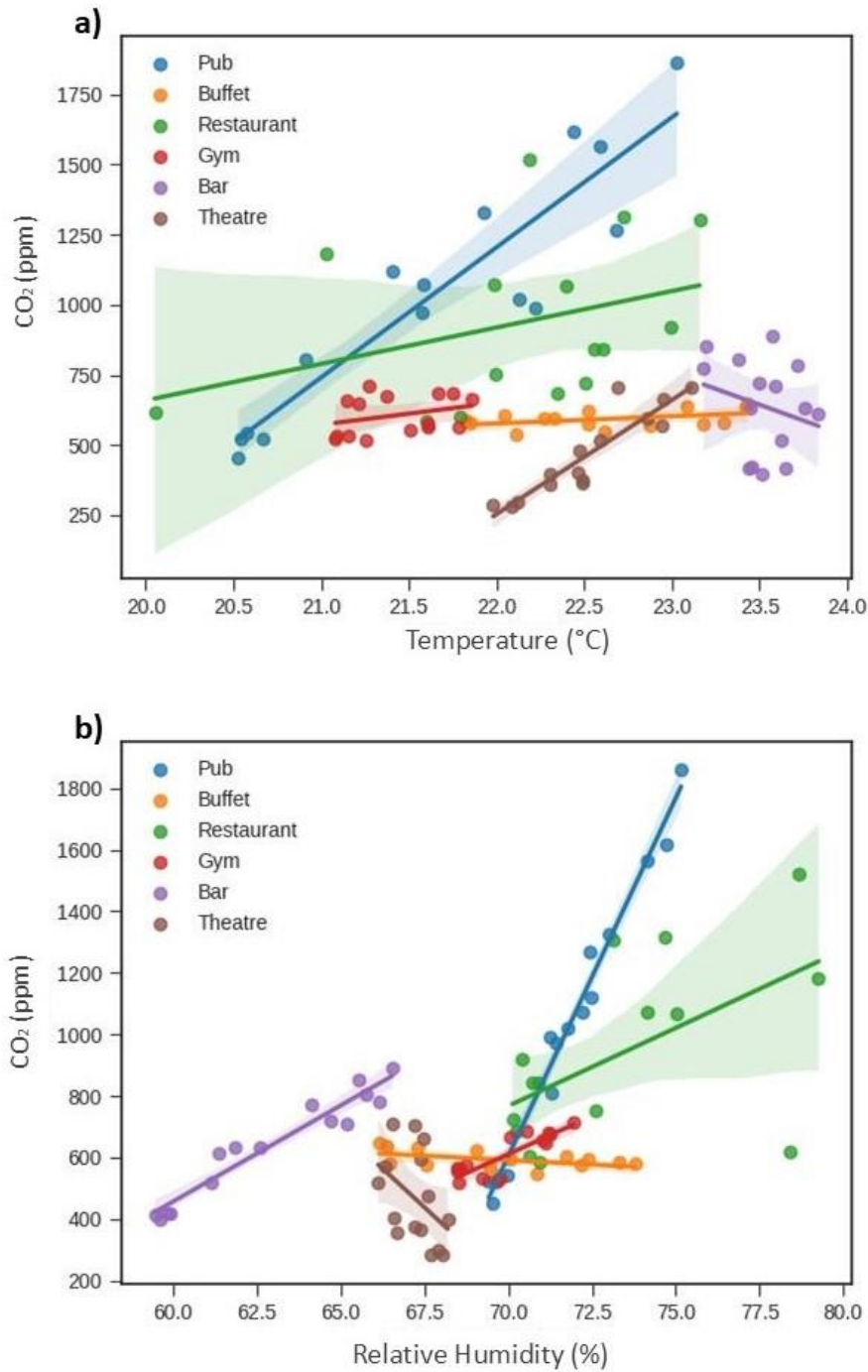


Figure 4. Scatter plots showing CO₂ concentration versus thermal comfort parameters in mass-gathering areas (exclude the three cabins, results for cabins are shown in Figure S7 on 21.08.2023 (sea day) during peak hours from 16:00-23:00h. (a) Temperature (°C) versus CO₂ concentration (ppm). (b) Relative humidity (%) versus CO₂ concentration (ppm). The scattered data points represent data in a half-hourly average, the solid lines are the regression lines and the shaded areas indicate the confidence interval (level 95%).

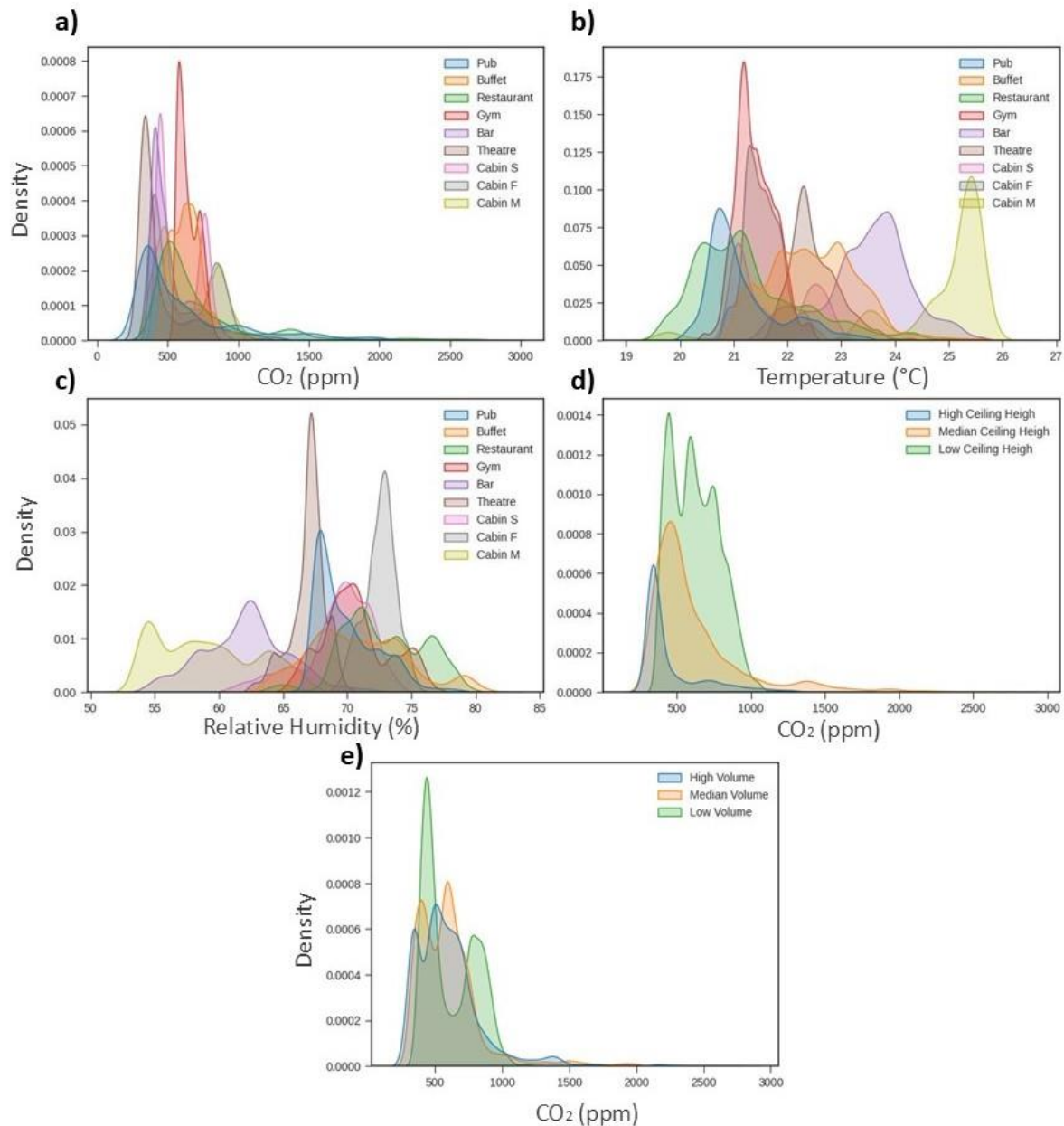


Figure 5. Kernel density distribution plots for the identification of occurrence frequency: (a) Density plots of the averaged CO₂ concentrations for all monitored locations; (b) Density plots of temperature for all monitored locations; (c) Density plots of RH for all monitored locations; and density plots of averaged CO₂ concentrations in contrast with different ship design conditions: (d) Volume of venue, (e) Deck ceiling height.

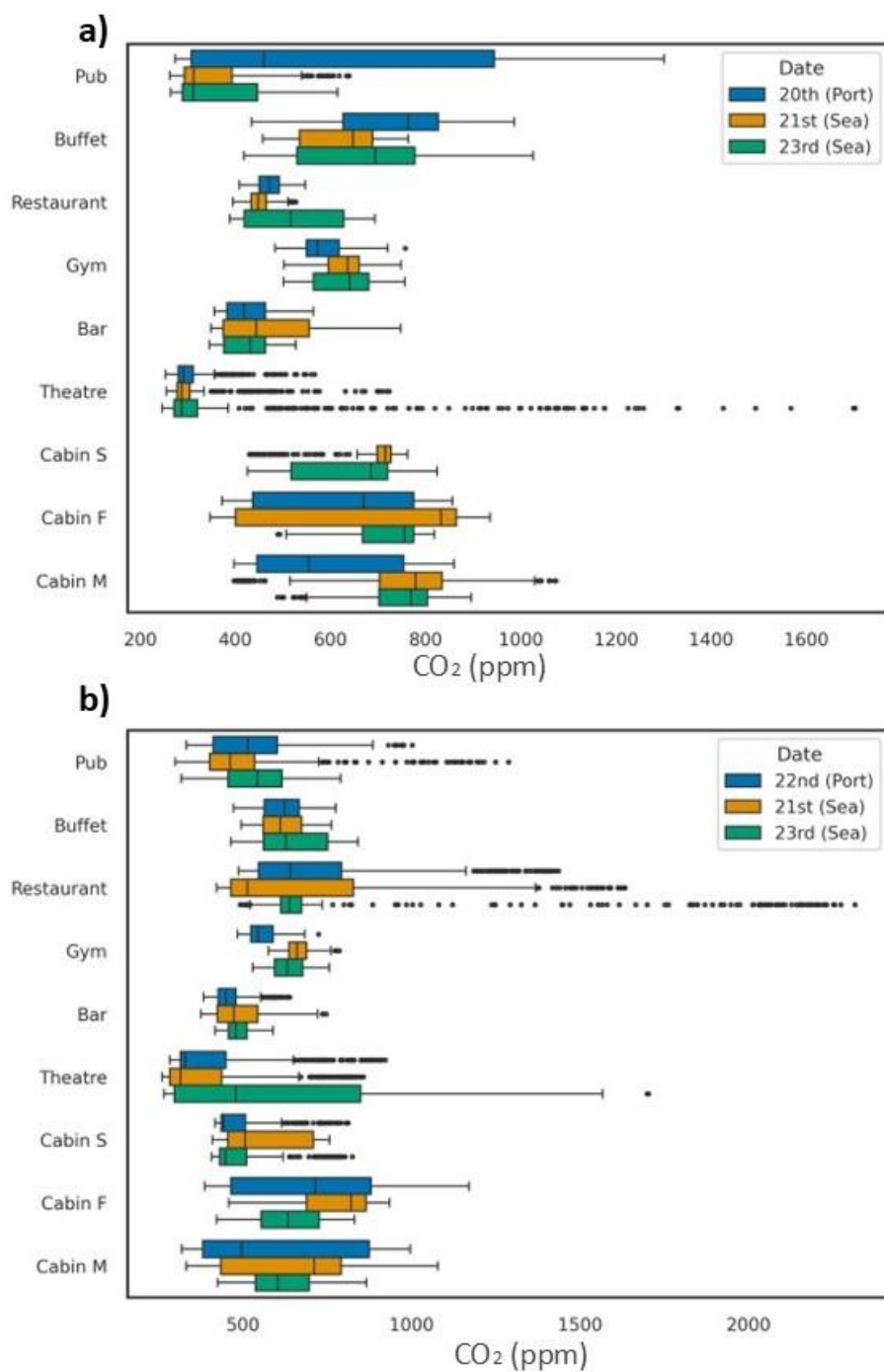


Figure 6. Comparison to the variation of CO₂ concentrations on board the cruise ship for the 21st and 23rd (sea day), 20th and 22nd (port day) of August 2023. (a) Variation of CO₂ concentrations on the 20, 21 and 23.08.2023. (b) Variation of CO₂ concentrations on the 21-23.08.2023.

List of Tables

Table 1. Description of monitoring locations, durations and the total hours of monitoring for all monitored locations.

No.	Monitoring locations	Monitoring duration		Total monitoring hours
		Start time ^d	End time ^d	
1	Buffet	16.08.23 22:30	24.08.23 01:45	171.25
2	Gym	17.08.23 01:30	24.08.23 00:00	166.5
3	Bar	17.08.23 01:30	23.08.23 23:57	166.45
4	Restaurant	17.08.23 02:30	24.08.23 00:03	165.55
5	Pub	19.08.23 20:00	24.08.23 00:07	100
6	Theatre	19.08.23 20:00	23.08.23 23:25	99.25
7	Cabin M ^a	19.08.23 01:30	24.08.23 07:38	126.13
8	Cabin F ^b	19.08.23 01:30	24.08.23 07:34	126.07
9	Cabin S ^c	20.08.23 22:00	24.08.23 06:45	80.75

^aMale cabin. ^bFemale cabin. ^cSingle occupant male cabin. ^dlocal time. Note: cabins M, F and S were reserved for the research team on board instead of the general guests; 21 and 23.08.2023 are sea days.

Table 2. Description of monitoring location characteristics, including maximum occupancy, ceiling height, floor area and volumes.

Monitoring locations	Maximum occupancy	Ceiling height (m)	Floor area (m ²)	Volume (m ³)	Deck (level)
Buffet	306	2.74	1217	3333.6	15
Gym	50	2.85	570	1624.4	16
Bar	180	3.2	630	2015.9	18
Restaurant	598	3	1050	3150	5
Pub	81	3.67	200	733.7	7
Theatre	945	6.25	1000	6249.5	5 & 6
Cabin M	2	2.74	17	46.3	13

Cabin F	2	2.74	10	27.2	13
Cabin S	2	2.74	17	46.3	11

1361

1362 **Table 3.** Recommended targets for CO₂, VR, temperature and RH for indoor spaces.

	Issuing authority and organisation				
Parameter	CIBSE _a	ASHRAE	REHVA _d	SAGE - UK _e	HSE - UK _f
CO ₂ (ppm)	800 - 1000	1000 _b	-	1500	-
VR (L s ⁻¹ person ⁻¹)	10	7.5 _b	10	-	-
Temperature (°C)	-	21 - 23 _c	-	-	> 16
RH (%)	-	40 - 60 _c	-	-	-

1363 ^aCIBSE, 2021. ^bASHRAE, 2023. ^cASHRAE, 2013. ^dREHVA, 2021. ^eEMG and SPI-B, 2021.

1364 ^fHSE, 2024.

1365

1366 **Table 4.** Estimated mean and standard deviation (STD) for ACH and VR at all monitored
1367 locations.

Sites	ACH (h ⁻¹) mean ± STD	VR (L s ⁻¹ person ⁻¹) mean ± STD
Buffet	0.8 ± 0.6	9.1 ± 6.5
Gym	0.5 ± 0.2	15.8 ± 7.8
Bar	1.7 ± 0.5	19.1 ± 5.1
Pub	2.3 ± 0.9	20.6 ± 7.8
Restaurant	0.8 ± 0.4	4.3 ± 2.2
Theatre	13 ± 11.1	86 ± 73.3
Cabin F	1.66 ± 1.1	22.6 ± 15.1
Cabin M	3 ± 1.5	69 ± 34
Cabin S	1.5 ± 0.6	35.5 ± 14.1

1368